AMPHETAMINE-INDUCED CHANGES IN AROUSAL AND LOCOMOTION AND THEIR EFFECTS IN NEURAL SIGNALING IN THE RETROSPLENIAL CORTEX

REBECA LEON PARADA
Bachelor of Science in Physics, **Universidad de Los Andes, 2017**

A thesis submitted
in partial fulfilment of the requirements for the degree of

MASTER OF SCIENCE

in

NEUROSCIENCE

Department of Neuroscience
University of Lethbridge
LETHBRIDGE, ALBERTA, CANADA

AMPHETAMINE-INDUCED CHANGES IN AROUSAL AND LOCOMOTION AND THEIR EFFECTS IN NEURAL SIGNALING IN THE RETROSPLENIAL CORTEX

REBECA LEON PARADA

Date of Defense: August 26, 2021

Dr. Aaron Gruber	Associate Professor	Ph.D.
Thesis supervisor		
Dr. Artur Luczak	Professor	Ph.D.
Thesis Examination Committee		
Dr. Masami Tatsuno	Professor	Ph.D.
Thesis Examination Committee		
Dr. Ian Whishaw	Professor	Ph.D.
Chair, Thesis Examination Committee		

Abstract

Changes in neural activity induced by amphetamine (AMPH) are thought to be a direct effect of the drug. However, this may be an artifact of motoric output and/or arousal. Here, we used a model of chronic AMPH taking to provide evidence that variations in retrosplenial cortex (RSC) activity are attributable to changes in running speed and pupil area. We show that speed is the best predictor of the average neural activity variance, whereas pupil area makes smaller contributions. Moreover, we found that the relationship between these parameters and neural activity is unaltered during AMPH administration or discontinuation. In other words, AMPH evokes changes in neural activity by changing motoric output and arousal, and not by changing the sensitivity of neural activity to these. Our results provide evidence of the potential for psychostimulants to alter neural activity via movement, and they highlight the importance of motion tracking.

Acknowledgements

First and foremost, I want to express my gratitude to my supervisor, Dr. Aaron Gruber, for his support and guidance over the past two years. His help has been crucial not only to my research but also to my progression towards becoming a better scientist. I would also like to thank the members of my supervisory committee, Dr. Artur Luczak and Dr. Masami Tatsuno for their help and recommendations to this project. Moreover, I am wholeheartedly grateful to my defense chair, Dr. Ian Whishaw for his invaluable support and help throughout my graduate program.

I want to specially acknowledge the help I have received from various current and former members of the Gruber Lab: I am greatly grateful to Victorita Ivan for providing the data that was used in this research project, and to Leonardo Molina for his help and suggestions to the data analysis. Thanks to David Tomàs for his recommendations, and to Ashley Slingerland, Mansi Patel, Parker McNabb, and Tessa Carrels for their help with calcium imaging data preprocessing. This thesis would not have been possible without their contribution.

I would also like to express my gratitude to HaoRan Chang, and Milad Naghizadeh for reviewing the first draughts of the thesis proposal and introduction. Finally, thank you to my family and friends, who have supported me in my graduate journey and put up with me as I prepared my thesis, and to everyone who indirectly contributed to this research.

Table of Contents

List of Tables

List of Diagrams

List of Figures

List of Abbreviations

REM	Rapid Eye Movement
AMPH	Amphetamine
DA	Dopamine
NE	Norepinephrine
RSC	Retrospenial Cortex
GCaMP	Green Calcium Modulated Protein
GENIE	Genetically Encoded Neuronal Indicator and Effector Project
SNR	Signal-to-noise ratio
PFC	Prefrontal Cortex
PPC	Parietal Cortex
DMS	Dorsomedial Striatum
ACC	Anterior Cingulate Cortex
mPFC	Medial Prefrontal Cortex
DAT	Dopamine transporter

Chapter 1: Introduction

The brain can be thought of as a dynamic system in a multidimensional space. In this context, '*state'* refers to a point where the position along each dimension can correspond to the activity of either a neuron, neuronal population, or brain region. Constantly varying activity appears as a trajectory in this state space (McCormick, Nestvogel et al. 2020).

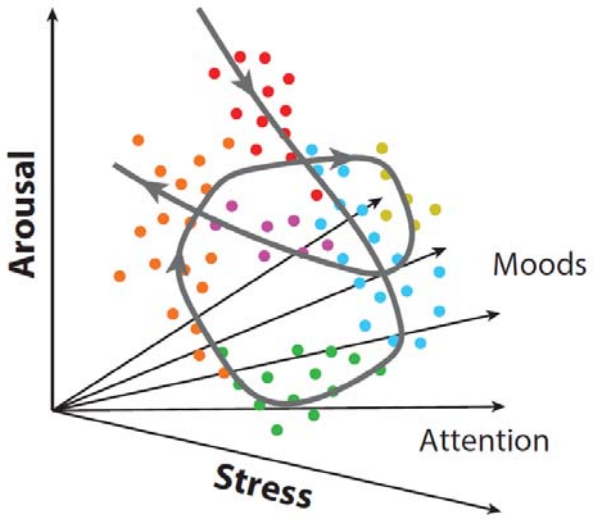

Figure 1. Brain activity wanders between states in a high-dimensional space. Certain locations are visited much more frequently than others, forming clouds of preferred states (coloured dots) and preferred trajectories through these states (McCormick et al., 2020).

In the late twentieth century, many scientists believed that brain states were a function of the sleep-wake cycle. Only certain patterns of activity associated with these two states were well-characterized: strong low-frequency fluctuations in cortical activity during slow-wave sleep ("synchronized" state); and suppression of low frequency fluctuations during waking and a special

sleep state associated with rapid eye movement (REM; "desynchronized" state) (Steriade, McCormick et al. 1993, Contreras, Timofeev et al. 1996, McCormick and Bal 1997, Destexhe, Contreras et al. 1999, Steriade, Timofeev et al. 2001). This classical view was debunked when advances in imaging technology led to the observation of variations within the waking state, which are tied to the behavioural context of the animal. Behavioural context relates to changes in arousal and motor activity. For example, previous work in awake mice has revealed that the cortex is desynchronized during bouts of exploratory behavior, such as whisking (Crochet and Petersen 2006, Gentet, Avermann et al. 2010, Zagha, Casale et al. 2013) and running (Niell and Stryker 2010, Bennett, Arroyo et al. 2013, Polack, Friedman et al. 2013, Saleem, Ayaz et al. 2013, Reimer, Froudarakis et al. 2014, Zhou, Liang et al. 2014), compared to stationary periods. The differences in cortical activity patterns found in these studies resemble the effects of focused spatial attention in primates (McAdams and Maunsell 1999, Cohen and Maunsell 2009, Mitchell, Sundberg et al. 2009, Harris and Thiele 2011).

Arousal and locomotion are altered in human substance abuse, and this is replicated in animal models. In particular, acute (on-board) amphetamine (AMPH) has arousal enhancing effects derived from its induced facilitation of monoamine transmission – especially dopamine (DA) and norepinephrine (NE) – (Haber, Barchas et al. 1981, Faraone 2018). Conversely, animal models of AMPH withdrawal are characterized by decreased locomotor activity, and decreased ability to alter concentrations of norepinephrine and dopamine (Paulson, Camp et al. 1991). Separate experiments have revealed that neural activity rates in the neocortex are increased by chronic AMPH administration (Contreras, Schjetnan et al. 2013), and decreased during cessation of drug administration (Lapish, Balaguer-Ballester et al. 2015, Belujon, Jakobowski et al. 2016, Hashemnia, Euston et al. 2020). The overarching **hypothesis for this thesis** is that much of the

change in neural activity evoked by AMPH administration or withdrawal is attributable to changes in arousal and locomotion states. To our knowledge, the relationship between activity and behavioural measures (arousal, locomotion) *during* AMPH consumption and withdrawal has never been studied before. Thus, our aim is to quantify how much variance in the retrosplenial cortex (RSC) is explained by arousal and speed, and to assess if the relationship between these parameters holds when psychostimulants are on-board, or when they are off-board but have been given multiple times in the past as a model of chronic drug taking.

1.1 The pupil as a measure of arousal

Several neuromodulatory pathways within the brainstem, thalamus, hypothalamus, and basal forebrain comprise the so-called 'ascending arousal system.' These broadly projecting pathways include cholinergic brainstem and basal forebrain nuclei, noradrenergic brainstem nuclei, serotonergic brainstem neurons, and histaminergic hypothalamic cells (Steriade 1996, Jones 2003). The size of the pupil is a well-established measure of a wide variety of mental and emotional factors related to the ascending arousal system activity, including arousal, attention, stress, and cognitive load (Hess and Polt 1960, Hess and Polt 1964, Kahneman and Beatty 1966, Poock 1973, Hoeks and Levelt 1993, Iriki, Tanaka et al. 1996, Bradley, Miccoli et al. 2008, Einhauser, Koch et al. 2010, Gilzenrat, Nieuwenhuis et al. 2010, Alnæs, Sneve et al. 2014, de Gee, Knapen et al. 2014). In addition, research in multiple species shows that fluctuations in pupil size are highly correlated with changes in brain states, neural responsiveness, and behavioural performance (Reimer, Froudarakis et al. 2014, McGinley, David et al. 2015, Vinck, Batista-Brito et al. 2015). Pupil size has also been shown to be a reliable indicator of activity in the locus coeruleus, which contains noradrenergic cells that project widely throughout the brain (Murphy,

Robertson et al. 2011, McDougal and Gamlin 2015, McGinley, David et al. 2015, Joshi, Li et al. 2016, Reimer, McGinley et al. 2016).

1.2 The retrosplenial cortex

The retrosplenial cortex (RSC) is an association region that integrates thalamic, hippocampal, and neocortical information (van Groen and Wyss 1992, Wyass and Van Groen 1992, Van Groen and Wyss 2003, Cenquizca and Swanson 2007, Sugar, Witter et al. 2011). RSC neurons are essential for spatial learning and memory, similar to hippocampus neurons (Sutherland, Whishaw et al. 1988, Vann and Aggleton 2005, Czajkowski, Jayaprakash et al. 2014). They carry various navigation-related signals such as head-direction, positional, and conjunctive allocentric and egocentric information (Chen, Lin et al. 1994, Cho and Sharp 2001, Smith, Barredo et al. 2012, Alexander and Nitz 2015, Alexander and Nitz 2017, Mao, Kandler et al. 2017, Vedder, Miller et al. 2017). RSC neurons also show spatial activity resembling the activity of hippocampal CA1 place cells. Mao and colleagues showed sparse, orthogonal, "place cell" sequence activity in RSC in a head-fixed locomotion assay, such as the one we used in this project (Mao, Kandler et al. 2017).

We recorded from the RSC for several reasons. First, it is easily accessible with two-photon imaging without removing tissue or implanting optics into the brain. Second, it is involved in spatial navigation, and is activated in head-fixed animals locomoting on a treadmill belt. Lastly, it receives noradrenergic innervation, and its afferents such as the medial prefrontal cortex and hippocampus are relatively rich in dopamine receptors. Therefore, RSC has properties useful for assessing the relationship between arousal/locomotion and neural activity, as well as the effects of AMPH on this.

1.3 Hypotheses

Our general hypothesis presented above can be resolved into three specific hypotheses. In particular: **(1)** a substantial amount of variance in the RSC can be accounted for by running speed and pupil area; **(2)** on-board AMPH will increase arousal and/or locomotor state, but not change the relationship between these states and neural activity (see diagram 1 with two possible scenarios); **(3)** AMPH discontinuation will cause hypo-arousal and decreased motoric output, but not change the relationship between these states and neural activity. The null hypothesis for #1 is that pupil size or running speed are unrelated to neural activity. There are two null hypotheses for #2-3. The first is that drug treatment has no effect on arousal and/or locomotion. The second is that drug treatments alter the relationship between arousal / locomotion and neural activity. To test these hypotheses, we combined pharmacology with two-photon imaging and pupil tracking in head-fixed mice running on a treadmill belt.

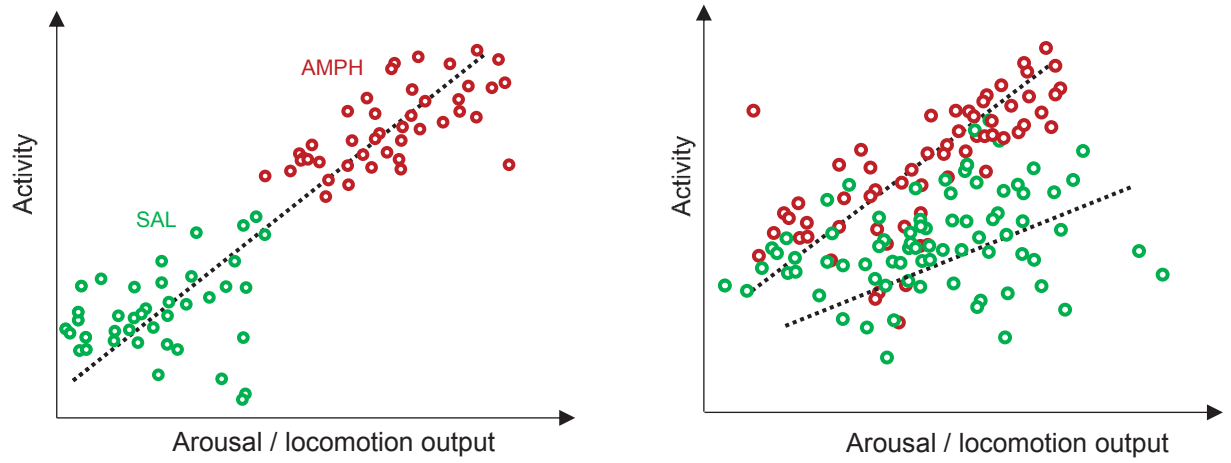

Diagram 1. Two possible scenarios showing the relationship between neural activity and behavioural metrics during AMPH consumption. Left: the relationship (slope) between arousal and/or locomotion and activity is not affected by the drug, but the drug exceeds the normal range of arousal / locomotion values. Right: AMPH changes the relationship between both parameters with a similar range of values as saline.

Chapter 2: Materials and methods

Note to readers. This is a data preprocessing and data analysis project. The data I am using has been collected by other members of the Gruber Lab.

2.1 Subjects

A total of 14 Thy1-GCaMP6s mice were used in this project. These transgenic mice, made by the Genetically Encoded Neuronal Indicator and Effector (GENIE) project, express the green, fluorescent calcium indicator (GCaMP6s) in the excitatory neurons of neocortical layers II, III and V. The 14 subjects were separated into two groups: (**1**) a saline group (n = 6), and (**2**) an amphetamine group (n = 8).

2.2 Surgical procedures

Mice were injected with dexamethasone (0.2 mg kg^{-1}; intramuscular injection) and a mixture of 5% dextrose and atropine (3 μg ml^{-1}; subcutaneous injection) two hours before being anesthetized with 1.5% isoflurane. Lidocaine (7 mg kg^{-1}) was injected subcutaneously under the incision site, and body temperature was maintained at 37° using a regulated infrared heating pad. A craniotomy was performed over the dorsal cortex, and a compound glass window was implanted and retained using tissue adhesive (Vetbond, 3M). The glass window was composed of a 7 mm diameter coverslip stacked over two 5 mm coverslips, held together with optical adhesive (NOA71, Norland). A custom titanium head-plate was attached to the skull with Metabond (Parkell) and dental adhesive. A rubber ring was fixed along the perimeter of the head-plate to retain distilled water during imaging and insulate the recording site from light contamination. Following surgery,

animals were single housed in clear plastic cages under a 12 h – 12 h reverse light cycle for a minimum of one week before the start of experiments. All procedures were performed in accordance with the Canadian Council of Animal Care and the Animal Welfare Committee at the University of Lethbridge.

2.3 Behavioural apparatus

After recovery from the surgery, water-restricted mice were habituated to head-fixation and underwent daily training to run over a linear treadmill. The treadmill belt was made with 150 cm of Velcro material (Country Brook), looped around two 3D printed polyamide wheels (10 cm diameter with centres separated by 40 cm). A photo-reflective tape was applied to one spot underneath the belt, which triggered a photoelectric sensor (Omron) that opened an electromagnetic pinch valve (Bio-Chem Valve) to dispense a 10% sucrose solution. The belt movement was monitored using a rotary optical encoder attached to the front wheel (Broadcom).

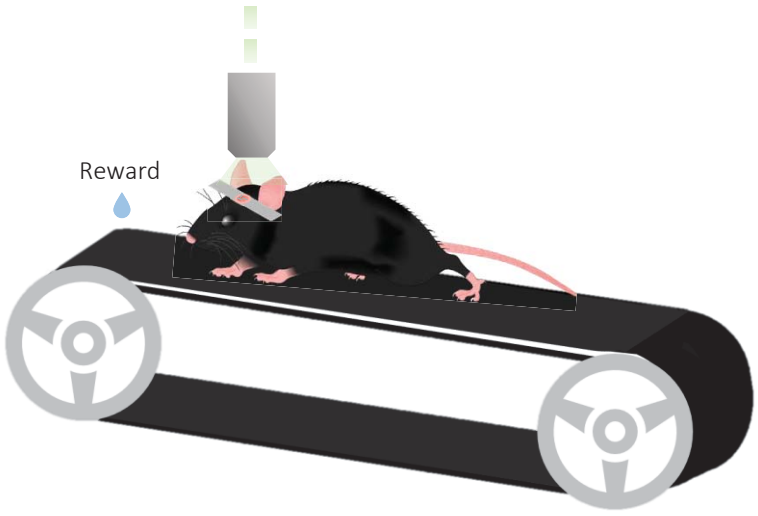

Figure 2. Behavioural apparatus: head restrained mice were trained to run over a 150 cm-long linear treadmill belt. For every lap covered they received a reward

2.4 Experimental design

After behavioural training, the two groups received either subcutaneous injections of saline (0.1 ml) or d-amphetamine hemisulfate for ten days. AMPH (Sigma-Aldrich, Ontario) was dissolved in 0.9% sterile saline and delivered following an escalating dose model (0.5 mg/kg, 1.0 mg/kg, 2.0 mg/kg), similar to previously studied animal models of drug abuse (Robinson and Kolb 1997). The imaging and behavioural recordings were made for two conditions: "on-board" (the drug was administered one hour before starting the recording, to ensure its effects), and "off-board" (the drug was administered after the recording) for each of the three doses.

Day 3:	**Day 5:**	**Day 7:**	**Day 9:**	**Day 11:**
AMPH 0.5 mg/kg	AMPH 1.0 mg/kg	AMPH 2 mg/kg	AMPH 2 mg/kg	AMPH 2 mg/kg
Drug ON	Drug ON	Drug ON	Drug ON	Drug OFF
Day 4:	**Day 6:**	**Day 8:**	**Day 10:**	**Day 12:**
AMPH 0.5 mg/kg	AMPH 1.0 mg/kg	AMPH 2 mg/kg	AMPH 2 mg/kg	AMPH 2 mg/kg
Drug OFF	Drug OFF	Drug OFF	Drug ON	Drug ON

Diagram 2. Study outline showing the experimental timeline and treatment schedule (amphetamine group). Day 1 and day 2 were baseline days. From days 3-12 animals received injections of AMPH.

2.4.1 Two-photon imaging

Gruber Lab performed two-photon imaging using a Thorlabs Bergamo II multiphoton microscope. A Ti-sapphire (Coherent) excitation laser operated at 920 nm was passed to the tissue through a 16× water immersion objective (Nikon, NA = 0.8, 80 – 120 mW). Laser scanning was controlled by a galvo-resonant scanner. The emitted GCaMP6 signals were amplified using a GaAsP photomultiplier tube (Hamamatsu) and digitized to a resolution of 800 × 800 pixels at a

sampling rate of 19 Hz. We imaged an 835 ×835 μm window over layers II–III of the agranular RSC at depths between 100 and 200 μm. A strip of Velcro wrapped around the body of the objective was lowered to the level of the rubber ring to block ambient light.

2.4.2 Video recordings

To track changes in pupil size, images of the eye were recorded at 25 frames per second using a Raspberry Pi 3 System (Raspberry Pi Foundation). A timestamp (trigger time and frame number) was imprinted every time a reward was delivered.

2.5 Data preprocessing

2.5.1 Imaging preprocessing

We conducted the registration and identification of regions of interest (ROIs) semi-automatically using Suite2P (Pachitariu, Stringer et al. 2017). Neurons were manually selected based on the morphology of the ROIs and the presence of distinct calcium deflections in the fluorescence trace. An array of deconvolved traces (ROIs by timepoints) was obtained for each session. The Suite2P deconvolution algorithm is based on the work made by Friedrich and colleagues (Friedrich, Zhou et al. 2017).

Some of the calcium signals detected with calcium imaging may be fast and 'small', thus making it difficult to identify real signaling events due to an unavoidable signal noise. In particular, GCaMP6 has a high signal-to-noise ratio (SNR) that can cause the estimation of the baseline fluorescence (F_0) to be negative or near-zero. Because this could affect the results, it was decided to work with the raw deconvolved traces from Suite2P. Stringer and Pachitariu found that using

these deconvolved values gives the most reliable responses to stimuli (measured by signal variance) (Stringer and Pachitariu 2019).

2.5.2 Video preprocessing

Custom Python code was used to do the video preprocessing. First, we inverted the colours because the two-photon laser produced a corneal reflection that affected pupil detection. Then, we extracted the reward timestamps using the algorithm to scan each frame for text and writing a '.csv' file with the frame number and time of each reward.

2.5.3 Pupil segmentation

We performed post hoc pupil segmentation semi-automatically using Python code developed by Molina (https://github.com/leomol). For the computation, the largest cluster of pixels is subtracted from the ROI. The algorithm zeros out any pixel less than a threshold – which can be changed to adjust for brightness changes – and fits the pupil to an ellipse. Many ROIs can be drawn across the video frames to account for movement changes.

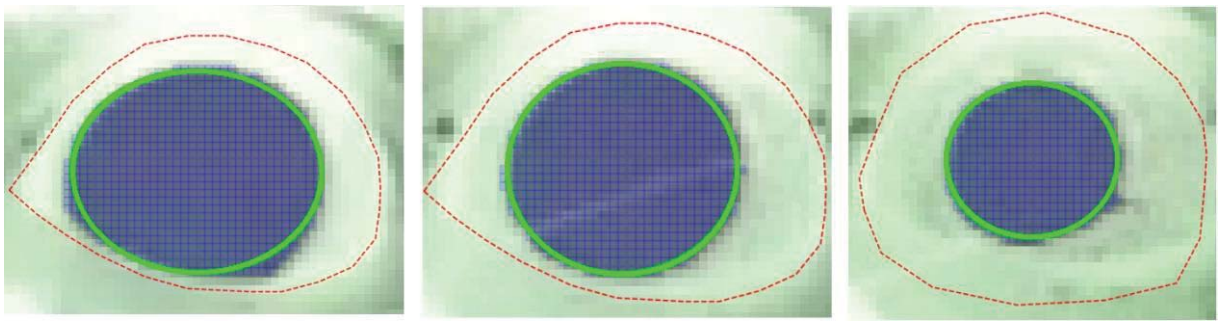

Figure 3. Video frame images of the mouse's eye. Pupil area was recorded on video and extracted post hoc via a fitted ellipse (green). The red dash line corresponds to the ROI.

2.6 Analysis

We used a total of 69 sessions for $n = 8$ mice ($n = 4$ mice from saline group; $n = 4$ from amphetamine group) divided according to the animal group and treatment schedule (on-board; off-board). Some of the data were excluded from the analysis because of the quality of the videos or because of problems with the behavioral recordings. Data were analyzed using MATLAB (The Mathworks Inc. Version 2018b) and resampled at 50 Hz, so that pupil area, neural activity, and position had the same sampling rate and length.

Table 1. Division of sessions for analysis according to group and treatment schedule

Group – treatment schedule	Number of sessions	Days
Saline on-board	19	3, 5, 7, 10 and 12
Saline off-board	15	4, 6, 8, 11
Amphetamine on-board	20	3, 5, 7, 10 and 12
Amphetamine off-board	15	4, 6, 8, 11

2.6.1 Smoothing

Pupil area traces were smoothed by computing the median over a .5s sliding window using MATLAB's function '`smoothdata`.' Running speed was computed using the linear position, and a smoothed version was obtained by computing the median over a 3s sliding window. To obtain the mean activity per session, deconvolved traces from Suite2P were averaged, resulting in a single trace of n observations. Activity traces were smoothed over a 3s Gaussian-weighted moving window.

2.6.2 Location specificity of cells

To generate the lap-to-lap position activity maps, we followed the methods of Mao and colleagues (Mao, Kandler et al. 2017): the 150-cm track was divided into 50 position intervals or bins, and the activity was averaged over the position bins. The results were normalized by the occupancy (i.e., divided by the number of samples) in each position bin. Data were filtered using a Gaussian smoothing window with 4.5 cm s.d. width.

2.6.3 Pearson's correlation

We divided the data into 4 distinct epochs to compute the linear correlation between pupil to mean activity, and speed to mean activity:

- Quiescence periods are defined as periods of 3 seconds before the locomotion onset, in which the animal had movement velocity of 0.1 cm/s or less.
- Locomotion periods are defined as periods of 7 seconds in which the animal had at least 5 cm/s.
- Reward approach phase is defined as the period of 4 second previous to the reward delivering, i.e., from -5 to -1 s.
- Reward consumption phase is defined as the period of 4 seconds after the reward delivering (including it), i.e., 0 to 4 s.

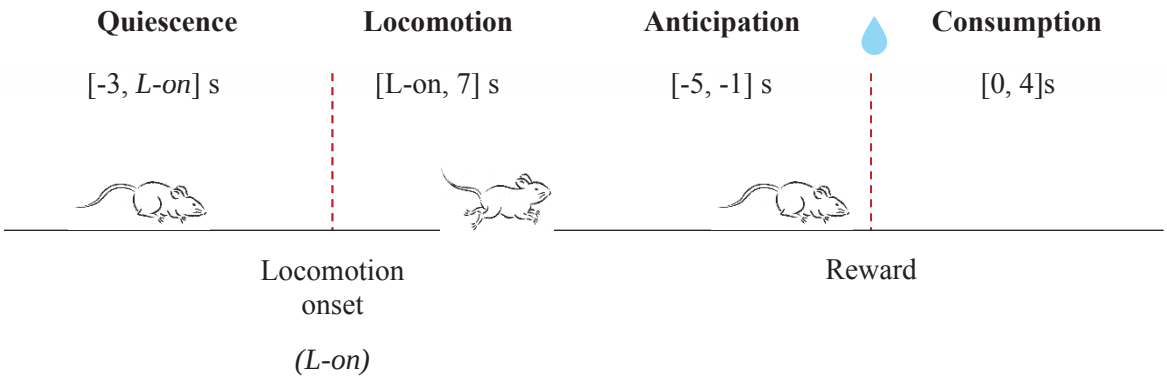

Diagram 3. Schematic showing division of data into epochs for analysis.

2.6.4 Regularization: Ridge regression

We wanted to build a linear model from the trend of the data to account for its variability. Ridge regression is a method for estimating coefficients of linear models that include correlated predictors (such as pupil area and running speed). Coefficient estimates for multiple linear regression models rely on the independence of the model terms. When terms are correlated and the columns of the design matrix X have an approximate linear dependence, the matrix $(X^T X)^{-1}$ is close to singular. Therefore, the least-squares estimate:

$$\hat{\beta}_{OLS} = (X^T X)^{-1} X^T Y \tag{2.1}$$

is highly sensitive to random errors in the observed response Y, producing a large variance. The general solution to this is reduce the variance at the cost of introducing some bias**.** This approach is called regularization. Specifically, in Ridge Regression, the ordinary least-squares loss function is augmented in such a way that it not only minimizes the sum of squared residuals, but also penalizes the size of parameter estimates, in order to 'shrink' them towards zero.

$$J = (X\beta - Y)^T(X\beta - Y) + \lambda\beta^T\beta \quad (2.2)$$

Solving (2.2) for $\hat{\beta}$ gives the Ridge regression estimates:

$$\hat{\beta}_{Ridge} = (\mathrm{X^T X} + \lambda \mathrm{I})^{-1}\,\mathrm{X^T Y} \quad (2.3)$$

Where 'λ' is the Ridge parameter and 'I' is the identity matrix. Small, positive values of λ improve the conditioning of the problem and reduce the variance of the estimates. While biased, the reduced variance of Ridge estimates often results in a smaller mean squared error when compared to least-squares estimates.

We performed a Ridge regression following the methods of Musall and colleagues to estimate the regression coefficients (Musall, Kaufman et al. 2019); repository available at: https://github.com/musall/ridgeModel. Their implementation chooses the penalty parameter (λ) using the fast marginal likelihood algorithm of Karabatsos (Karabatsos 2018). The response (dependent) variable corresponds to the mean neural activity of each session. The model's design matrix included several features, such as running speed, pupil size, position, time to reward and time after reward.

2.6.5 Cross-validated explained variance

To evaluate how well the model captured neural activity, we computed the 10-fold cross-validated explained variance ($\mathrm{cvR^2}$). The explained variance or $\mathrm{R^2}$ quantifies the relationship between responses and prediction by computing the correlation between them. Cross-validation ensures that no variation is predicted by chance, regardless of the number of model variables. To compute all the explained variance by individual model variables, we created reduced models

where all variables apart from the specified one were shuffled in time. The explained variance by each reduced model revealed the maximum potential predictive power of that corresponding model variable.

2.6.6 Statistics

Statistical significance was determined by three-factor mixed (one between and two within-subjects factors) repeated measures analysis of variance (ANOVA). We performed the repeated measures ANOVA using SPSS, which computes the adjusted *p*-values for when sphericity is not satisfied. We estimated marginal means and compared group means with post hoc pairwise comparison tests using the Bonferroni correction ($\alpha = .05$). We ensured that the amount of data used to perform this statistical analysis were enough to obtain meaningful results. We used a total of $n = 8$ animals and each one had at least 4 repeated 'on-board' and 'off-board' measurements divided into 50 intervals (bins) of time.

Chapter 3: Results

3.1 Single session analysis

We first sought to assess the changes in neural activity, running speed, and pupil area in one experimental session. This allowed us to establish relationship patterns to later quantify how much of the variance in neural activity was explained by arousal and movement separately. To briefly review the behavioural-task design, we combined a head-fixed locomotion assay with two-photon imaging and pupil tracking. Thy1-GCaMP6s mice were trained to run on a treadmill belt and received a sucrose reward upon each lap of the belt.

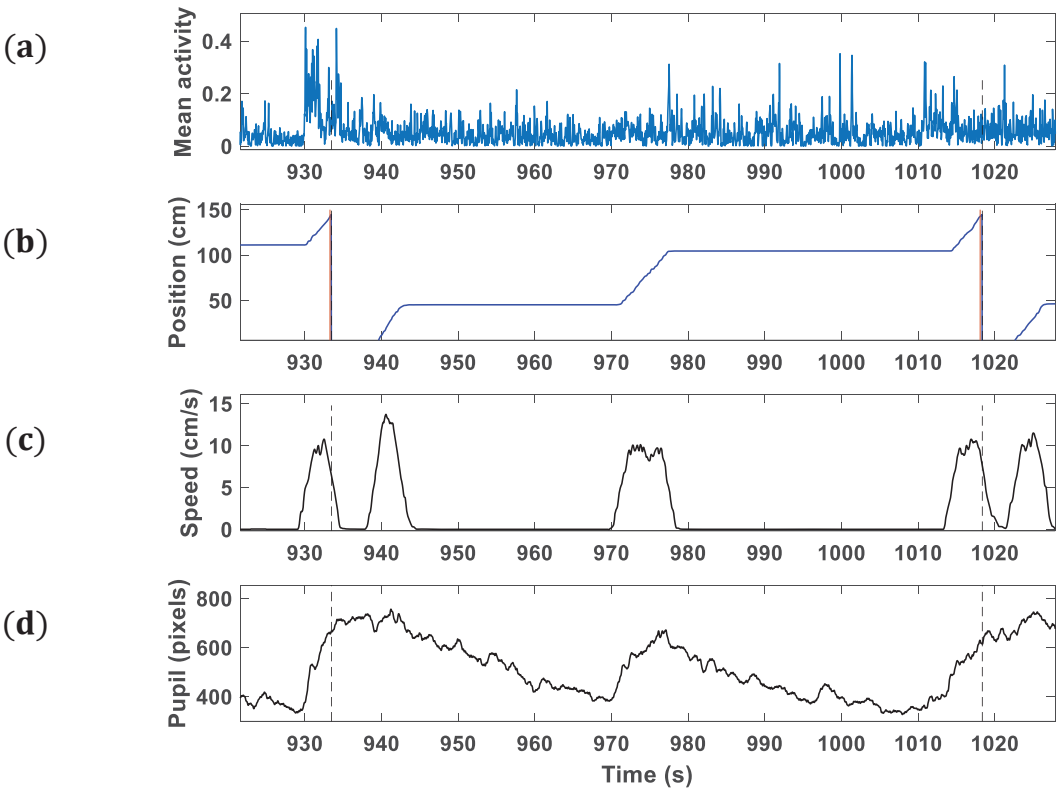

Figure 4. Example raw data from one experimental session (saline group) showing one complete lap. (**a**) Mean neural activity of all simultaneously recorded neurons (n = 260 cells for this example) (**b**) linear position of the belt (**c**) running speed (**d**) pupil area. The dotted line corresponds to trial onset.

Animals alternated between bouts of locomotion and pauses along the length of the belt, typically slowing down near the reward location. Moreover, there is some variability from trial to trial (figure 5).

Running speed and pupil area were consistently correlated during the experimental session (figure 6) as previously observed in moving animals (Reimer, Froudarakis et al. 2014, Vinck, Batista-Brito et al. 2015, Reimer, McGinley et al. 2016, Stringer, Pachitariu et al. 2019). Pupil area increased with locomotion onset and gradually decreased when the animal stopped moving, indicating a period of elevated arousal in the absence of locomotion (figure 4d).

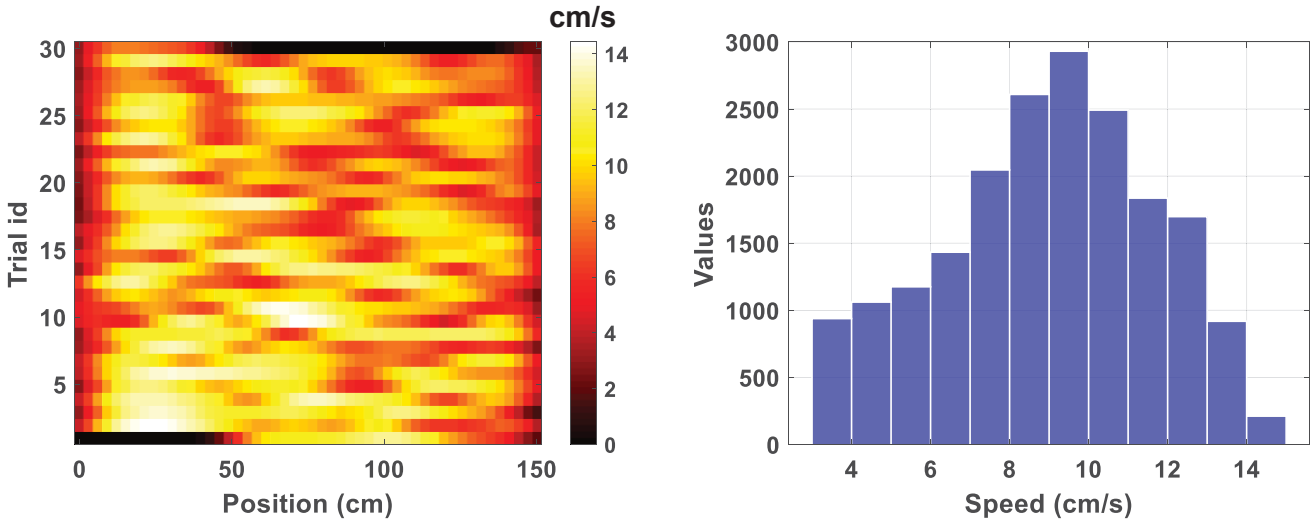

Figure 5. Lap running behaviour from one experimental session (saline group). Left: Movement speed as a function of location for 30 consecutive laps. The animal moved robustly and paused most frequently near the reward site (as shown by darker colours). Right: Histogram of running speed in between reward events.

Likewise, both running speed and pupil area were correlated with neural activity throughout the session (figure 6). There was an increase in neural activity and pupil size with locomotion onset, but unlike pupil area, neural activity decreased shortly after, even though the animal continued to move (figure 4a).

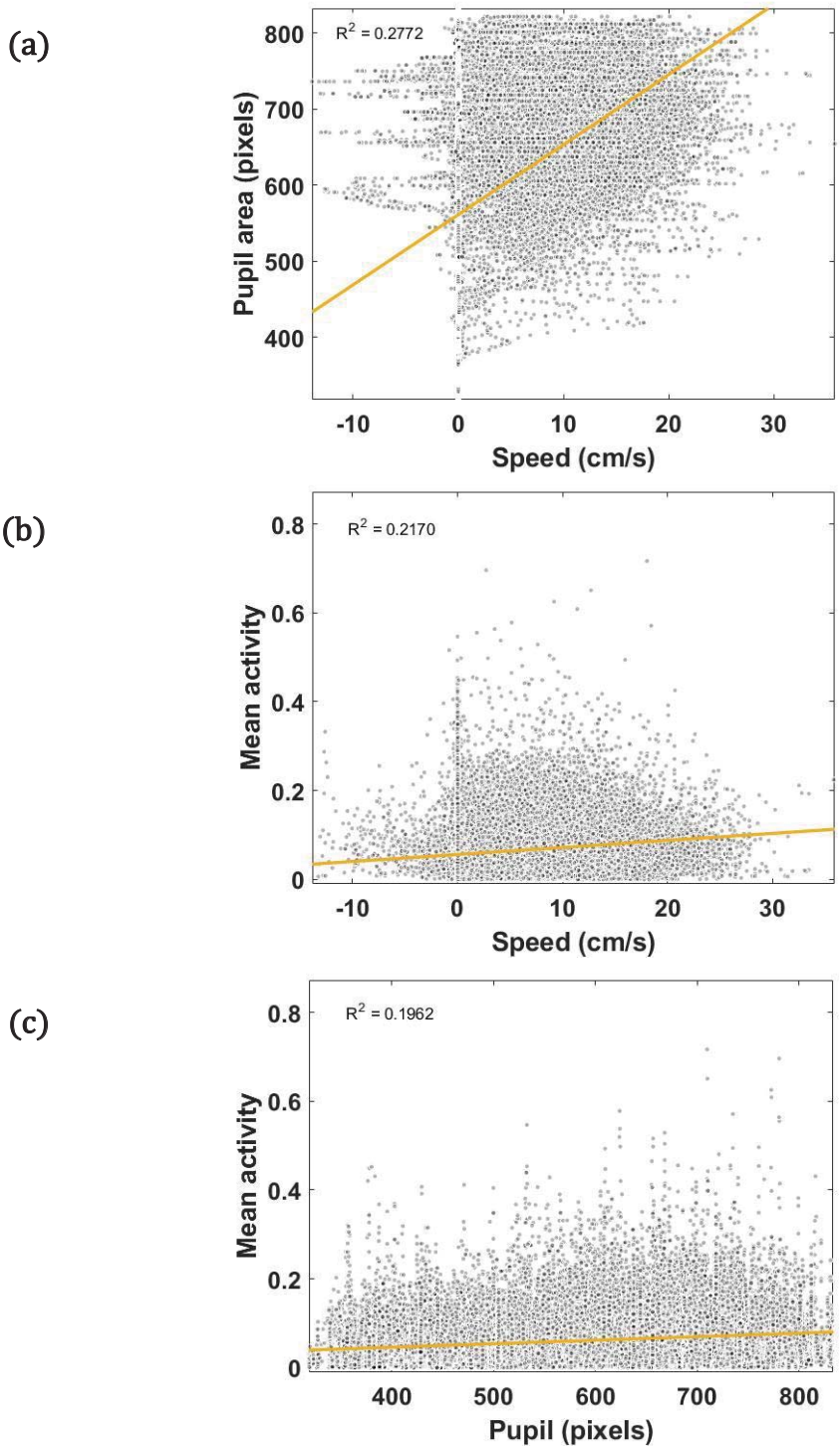

Figure 6. Scatter plots for one experimental session (saline group). (a) Running speed as a function of pupil area. (b) Pupil area and (c) running speed as a function of mean neural activity. Pupil area was correlated with running speed ($R^2 = 0.2772$). Both behavioural measures were also correlated with mean neural activity (speed to mean activity $R^2 = 0.2170$; pupil to mean activity $R^2 = 0.1962$).

Neural data also showed correlation with spatial location as previously observed in RSC cells (Mao, Kandler et al. 2017). We expressed neural activity as a function of the animal's location on the treadmill and averaged the result across laps.

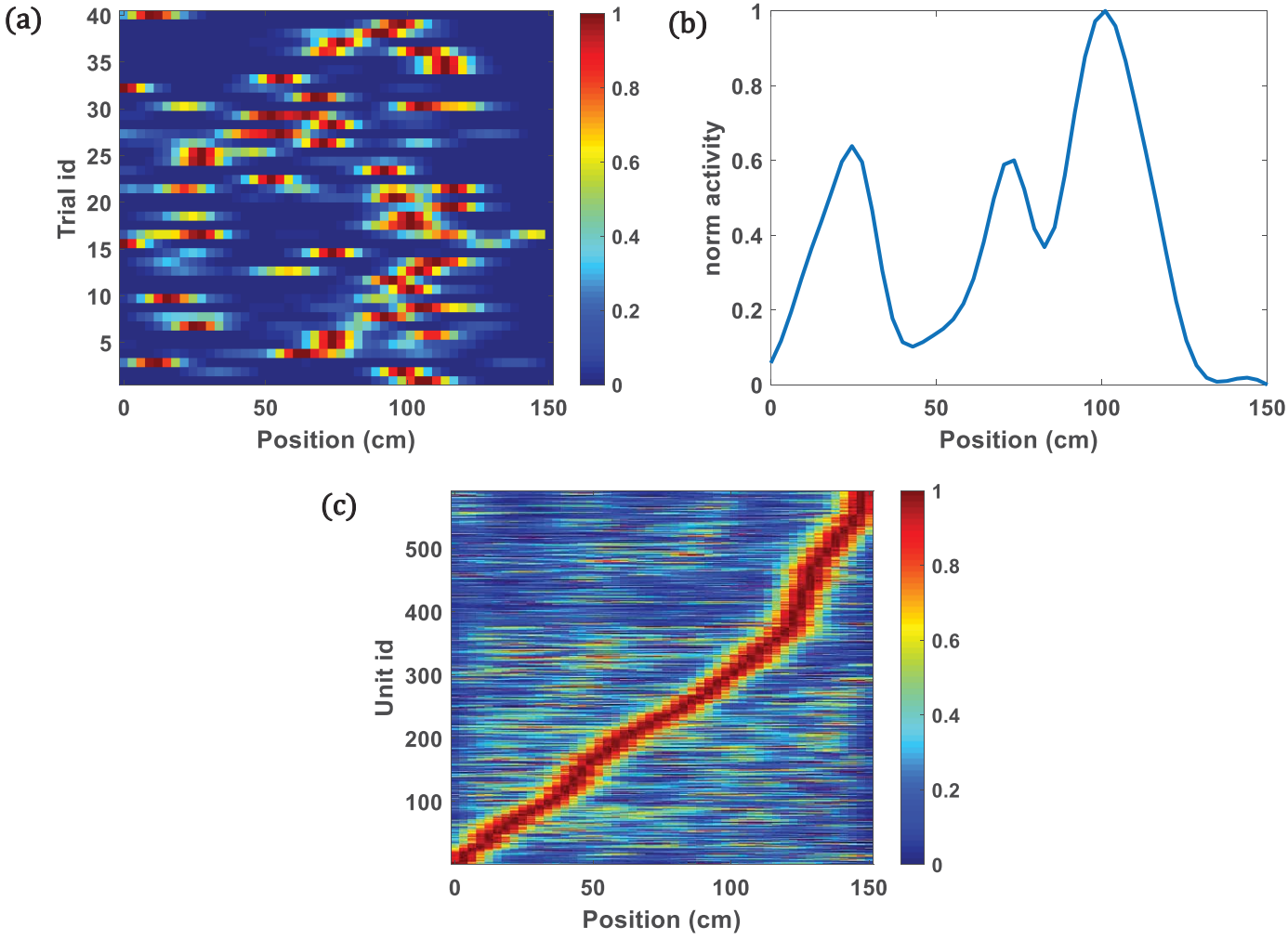

Figure 7. Location specificity of cells. (a) and (b) normalized activity of one representative cell as a function of location for 40 consecutive laps from one experimental session (amphetamine group). Note the repeated sequences of activation in specific locations on the belt. (c) Normalized activity as a function of location for all the 591 cells from the same experimental session. Cells were ordered by the positions of their peak average activity.

To further show the spatially localized firing of RSC cells, we took 2 subsets of trials and created the normalized activity plots as a function of location for all the cells. Each subset contains half of the trials. Both activity maps were made preserving the same order.

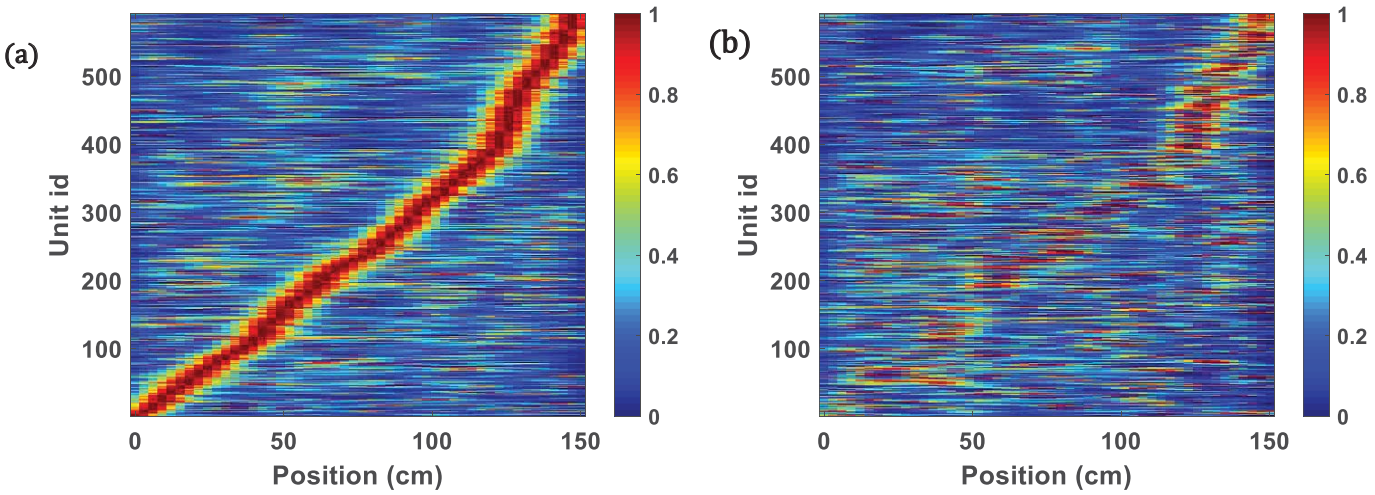

Figure 8. Normalized activity as a function of position (n = 591 cells) for the (a) first 20 trials and (b) last 20 trials.

Some of the pattern observed in the first half of the trial is preserved in the second half. There is a similar sequence of activation as the animal crossed distinct treadmill locations, especially when approaching the reward site. However, not all of these cells are place cells, and we did not use a criterion to classify them.

This single-session analysis has shown a relatively linear relationship between behavioural metrics and neural activity. We then sought to assess the effect of AMPH over group averaged data. To review the experimental design, animals were separated into two groups, and they received either saline or AMPH for ten consecutive days. Injections were delivered following a two-conditions treatment schedule: ‘on-board’ (administration), and ‘off-board’ (discontinuation).

3.2 Reward-triggered changes analysis

We assessed the potential effects of AMPH in mean neural activity, running speed and pupil area around reward delivery. To do this, we aligned the data to reward and showed changes during anticipation and consumption epochs. Our analysis suggests a similar modulation over the course of the trial in all of the variables: there is an increase as the animals approach the reward site, and then a decrease as they stop to consume the reward. The first part of the statistical analysis was made at reward delivery, which is the point when we expect monoamines to be released. Running speed is normalized across the groups, but there is still a difference in pupil area. We took a small window around reward delivery to look at whether that relates to any differences in mean neural activity.

Mean neural activity shows a decrease effect on the AMPH group compared to saline (figure 8a). According to a repeated measures ANOVA, around reward delivery there was no main effect of time ($F_{(2, 8)} = 1.283$, $p = .329$), treatment schedule ($F_{(1, 4)} = .040$, $p = .851$), group by time interaction ($F_{(2, 8)} = .461$, $p = .646$), or group by treatment schedule interaction ($F_{(1, 4)} = .246$, $p = .646$). However, the estimated marginal means is consistent with the effect we observe in the time traces (table 4), and a post hoc pairwise comparison using the Bonferroni correction ($\alpha = .05$) showed a significant difference in group ($p = .016$), and group by treatment schedule interaction ('on-board' $p = .011$; and 'off-board' $p = .041$).

Table 2. Mean neural activity across groups and treatment schedule conditions

Group * treatment

Group	treatment	Mean	Std. Error	95% Confidence Interval	
				Lower Bound	Upper Bound
'amphetamine'	1	.062	.004	.051	.073
	2	.059	.007	.040	.078
'saline'	1	.087	.004	.076	.098
	2	.088	.007	.069	.107

*'1' indicates 'on-board,' '2' indicates 'off-board.'

Running speed time traces show a remarkably similar profile as the mean neural activity during the anticipation phase (figure 8b). Around reward delivery, there was no main effect of time ($F_{(2, 8)} = .077$, $p = .927$) or treatment schedule ($F_{(1, 4)} = 6.056$, $p = .070$), but there was a significant interaction between group and time ($F_{(2, 8)} = 4.914$, $p = .041$). However, a post hoc pairwise comparison using the Bonferroni correction ($\alpha = .05$) did not show a significant difference in group when comparing across treatment schedules ('on-board' $p = .324$, 'off-board' $p = .459$).

Table 3. Mean running speed across groups and treatment schedule conditions

Group * treatment

Group	treatment	Mean	Std. Error	95% Confidence Interval	
				Lower Bound	Upper Bound
'amphetamine'	1	8.609	1.726	3.817	13.400
	2	10.294	2.368	3.720	16.869
'saline'	1	11.351	1.726	6.559	16.143
	2	13.037	2.368	6.462	19.612

*'1' indicates 'on-board,' '2' indicates 'off-board.'

The effect seen in mean neural activity and running speed is completely inversed in pupil area: AMPH groups tend to have larger pupil area values than the saline groups (figure 8c). A repeated-measures ANOVA around the reward delivery determined that mean pupil area values differed significantly across time ($F_{(2, 8)} = 5.611$, $p = .030$), treatment schedule ($F_{(1, 4)} = 16.950$, $p = .015$), and group by time interaction ($F_{(2, 8)} = 5.566$, $p = .031$).

The estimated marginal means showed an increase in pupil area values when comparing between group and treatment schedule conditions (table 2), and a post hoc pairwise comparison using the Bonferroni correction ($\alpha = .05$) showed a significant difference across groups and treatment schedules ($p = .047$ for 'on-board', $p = .017$ for 'off-board').

Table 4. Mean pupil area across groups and treatment schedule conditions

Group	treatment	Mean	Std. Error	95% Confidence Interval	
				Lower Bound	Upper Bound
'amphetamine'	1	827.290	85.361	590.290	1064.290
	2	905.102	71.367	706.956	1103.248
'saline'	1	728.505	85.361	491.505	965.505
	2	765.225	71.367	567.080	963.371

*'1' indicates 'on-board,' '2' indicates 'off-board.'

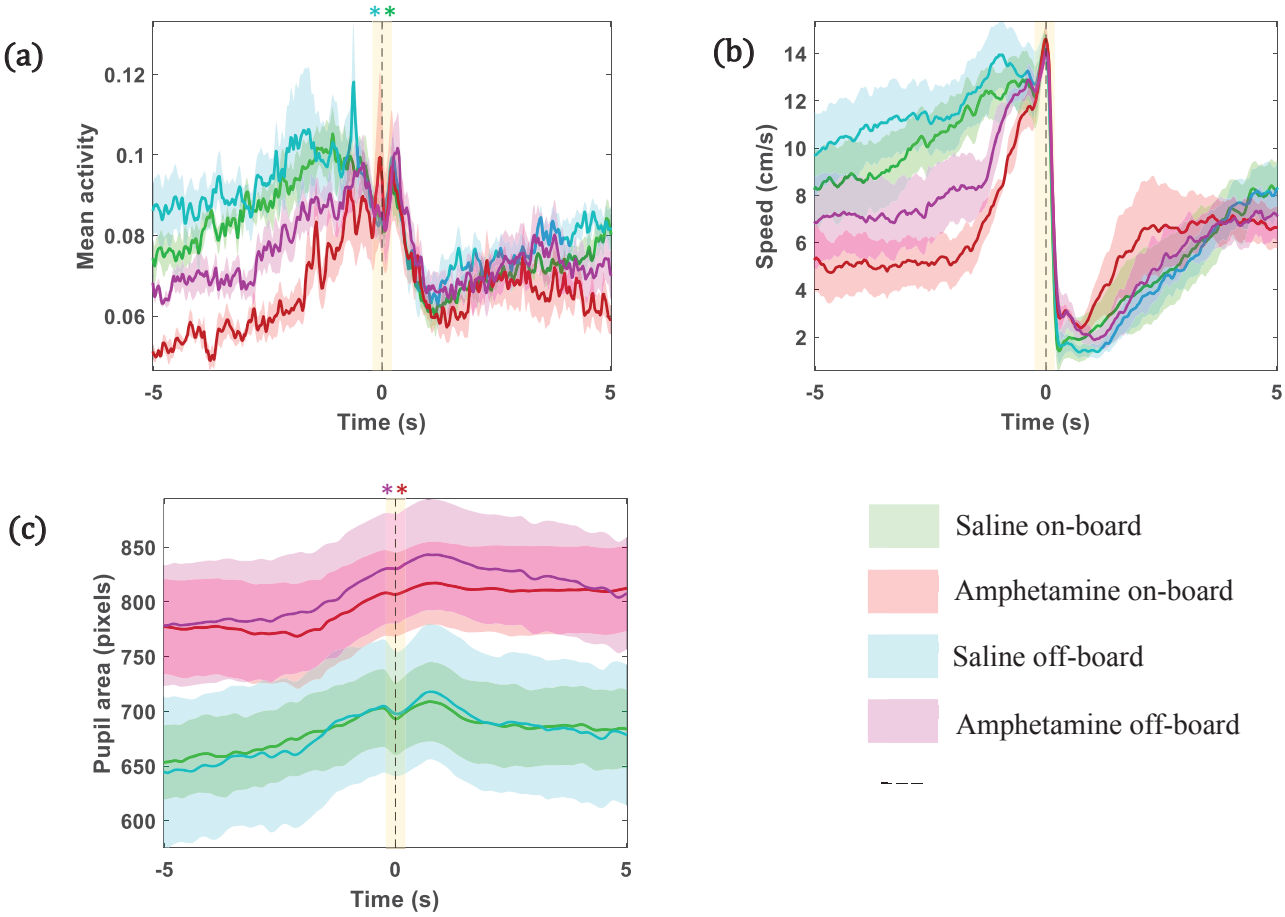

Figure 9. Group averaged data aligned to reward. (a) Mean neural activity, (b) running speed, and (c) pupil area. Shaded regions denote the standard error of the mean (s.e.m.). Asterisk represent group means that were significantly different from each other. Colour indicates the highest group mean for that treatment schedule condition.

We averaged all the data across the groups to look at differences in mean neural activity and running speed. This part of the statistical analysis was made on the entire data window. There is a significant effect of group on mean neural activity ($F_{(1, 3)} = 11.01$, $p = .051$), and according to a pairwise comparison test using the Bonferroni correction ($\alpha = .05$), the difference is significant ($p = .045$). There is also a significant effect of group on mean running speed ($F_{(1, 3)} = 12.17$, $p = .040$), and a significant difference according to the pairwise comparison test ($p = .039$).

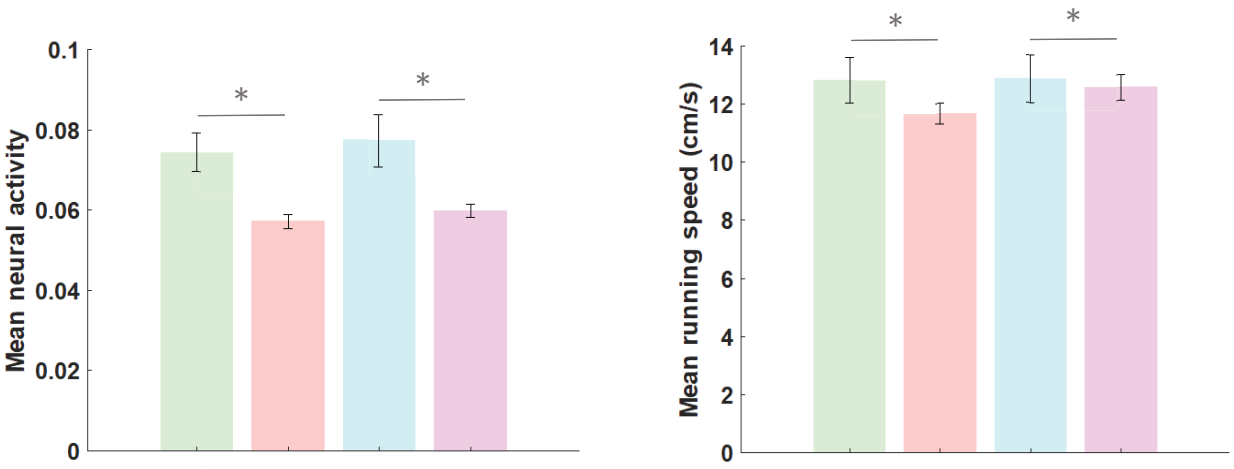

Figure 10. Group averaged data. (a) Mean neural activity, (b) mean running speed. Asterisks represent group means that were significantly different from each other.

We then grouped running speed time points into bins to look at the general representation of the data distribution. This analysis was made on the entire data window. Consistent with the time traces, the histograms suggest that the animals of the AMPH groups show more frequent off-task behaviors such as pausing.

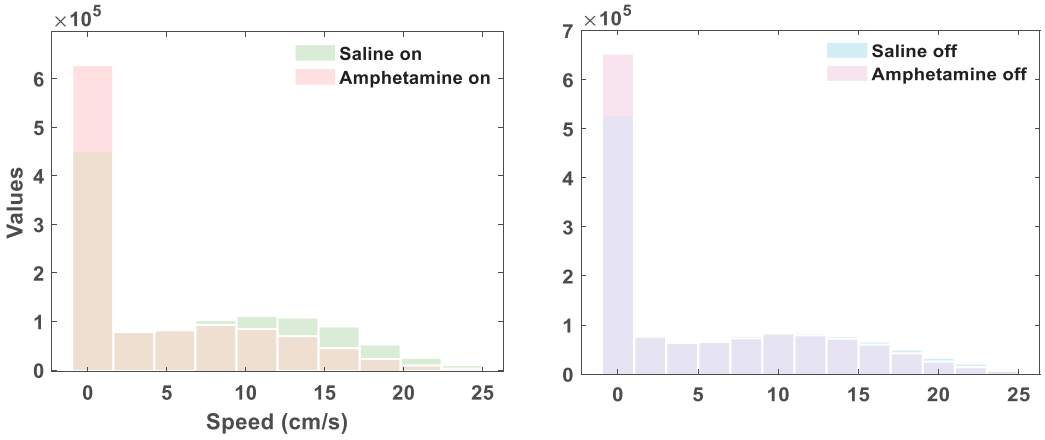

Figure 11. Histogram of group averaged speed.

3.3 Pearson's correlation

We studied the relationship between pupil area, running speed and neural activity during bouts of locomotion, periods of quiescence, and anticipation and consumption of reward (see diagram 3, Chapter 2). Running speed correlations were largely bigger than pupil area ones, and they tend to be higher for the AMPH group. However, this difference was not significant. Mean neural activity and pupil area were more correlated during quiescence, but according to a repeated measures ANOVA, there was no main effect or interaction. On the other hand, mean neural activity and speed were more correlated during approach, but there was no main effect or interaction either.

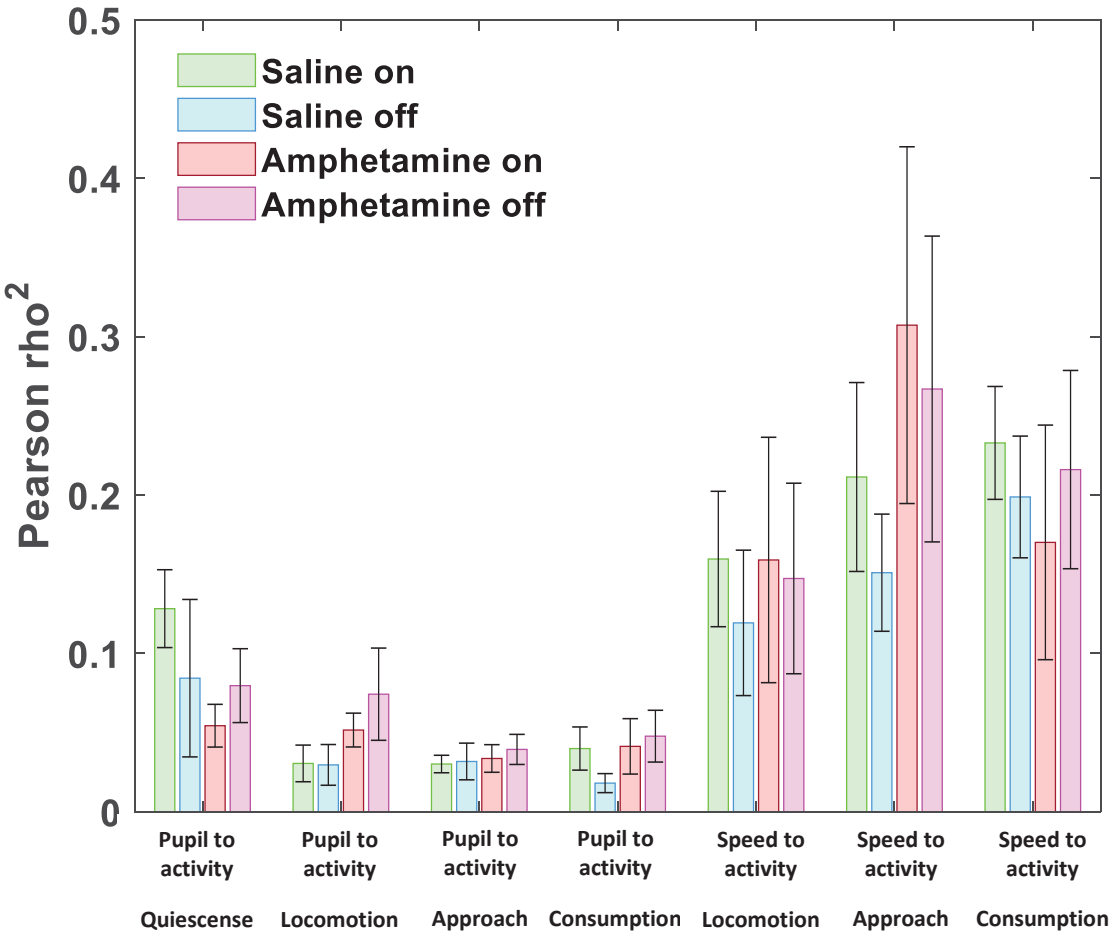

Figure 12. Pearson's correlation between pupil area, running speed and mean neural activity during distinct epochs.

Another way to look at these relationships and get the maximum predictive power of each behavioral measure is to compute the cross validated explained variance (cvR^2). To do this, we computed the correlation between the actual data values and the model predictions (built with the beta weights from the Ridge regression).

3.4 Ridge regression and cross-validated explained variance

We quantified the amount of neural activity in the RSC explained by behavioural measures. To do this, we fitted a Ridge regression model to our data. We used cross-validation to ensure that no variance is predicted by chance. By shuffling in time all parameters apart from the specified one, our Ridge model revealed the ability of that variable to explain the average variance of neural activity (explained variance).

Running speed and pupil area were the two best predictors of the average neural activity changes, followed by position, time to reward, and time after reward (figure 10). This is consistent with previous reports showing that movement (video, whisk, walk, eye movement) explains a high degree of neural activity (Musall, Kaufman et al. 2019, Stringer, Pachitariu et al. 2019, Salkoff, Zagha et al. 2020).

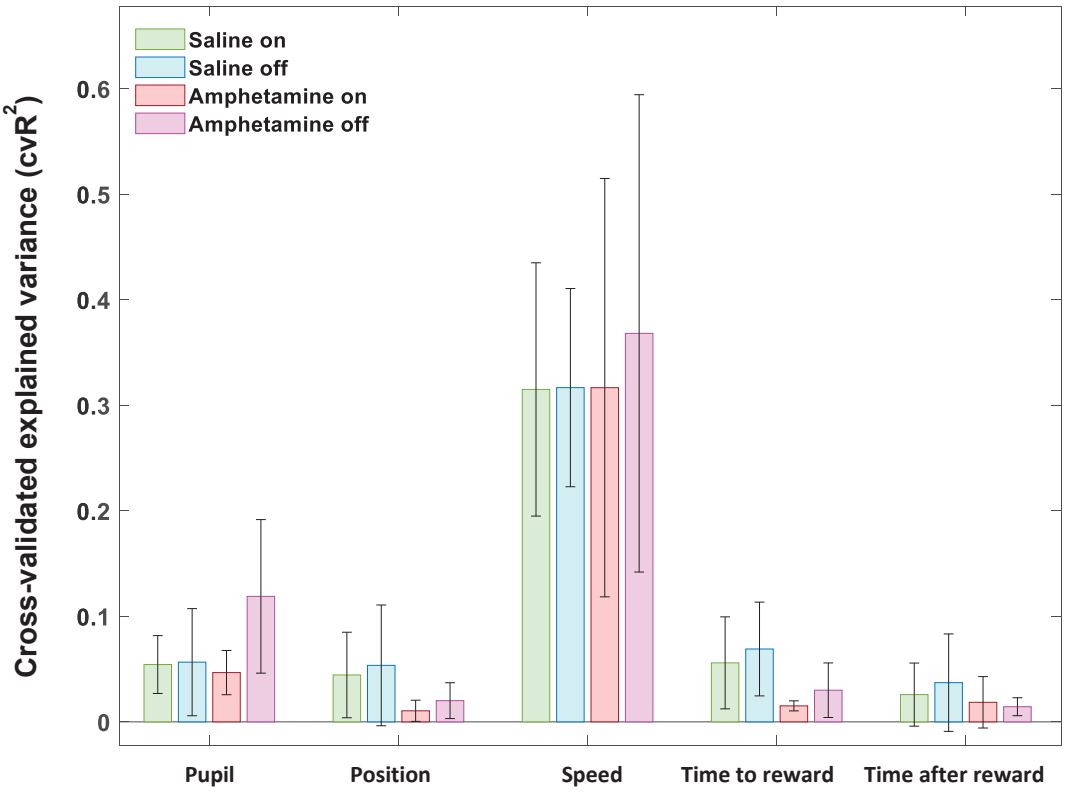

Figure 13. Unique explained variance for each behavioural measure.

Table 5. Cross-validated explained variance for each behavioural measure

Group-treatment schedule	**Pupil area** ($cvR^2 \pm$s.e.m.)	**Position** ($cvR^2 \pm$s.e.m.)	**Running Speed** ($cvR^2 \pm$s.e.m.)	**Time to reward** ($cvR^2 \pm$s.e.m.)	**Time after reward** ($cvR^2 \pm$s.e.m.)
Saline on	0.054 ± 0.027	0.044 ± 0.041	0.315 ± 0.120	0.056 ± 0.044	0.026 ± 0.030
Saline off	0.057 ± 0.051	0.054 ± 0.057	0.317 ± 0.094	0.069 ± 0.044	0.037 ± 0.046
Amphetamine on	0.047 ± 0.021	0.010 ± 0.010	$0.317 \pm .0198$	0.015 ± 0.005	0.019 ± 0.024
Amphetamine off	0.119 ± 0.073	0.020 ± 0.017	0.368 ± 0.226	0.030 ± 0.026	0.014 ± 0.009

Our statistical analysis did not show any significant main effect or interaction in the explained variance. In addition, the post-hoc tests using the Bonferroni correction ($\alpha = .05$) did not show a significant difference in group when comparing across treatment schedules.

We also performed post hoc pairwise comparison tests to compare the beta weights (slopes or regression coefficients) of pupil area and running speed for both groups and treatment schedule conditions. The tests did not show a significant difference in group or group by treatment schedule (table 6 & 7). These results indicate that amphetamine does not changes the relationship between arousal and locomotion metrics and neural activity. Between the different treatments, the drug does not affect the relationship between arousal / locomotion and neural activity.

Table 6. Pairwise comparisons of pupil area beta weights

treatment	(I) Group	(J) Group	Mean Difference (I-J)	Std. Error	Sig.[a]	95% Confidence Interval for Difference[a]	
						Lower Bound	Upper Bound
1	'amphetamine'	'saline'	-5.312E-8	.000	.889	-1.042E-6	9.360E-7
	'saline'	'amphetamine'	5.312E-8	.000	.889	-9.360E-7	1.042E-6
2	'amphetamine'	'saline'	-2.918E-7	.000	.393	-1.139E-6	5.558E-7
	'saline'	'amphetamine'	2.918E-7	.000	.393	-5.558E-7	1.139E-6

Group	(I) treatment	(J) treatment	Mean Difference (I-J)	Std. Error	Sig.[a]	95% Confidence Interval for Difference[a]	
						Lower Bound	Upper Bound
'amphetamine'	1	2	8.211E-8	.000	.737	-5.516E-7	7.158E-7
	2	1	-8.211E-8	.000	.737	-7.158E-7	5.516E-7
'saline'	1	2	-1.565E-7	.000	.530	-7.902E-7	4.772E-7
	2	1	1.565E-7	.000	.530	-4.772E-7	7.902E-7

Based on estimated marginal means

a. Adjustment for multiple comparisons: Bonferroni.

Table 7. Pairwise comparisons of running speed beta weights

treatment	(I) Group	(J) Group	Mean Difference (I-J)	Std. Error	Sig.[a]	95% Confidence Interval for Difference[a]	
						Lower Bound	Upper Bound
1	'amphetamine'	'saline'	-1.363E-5	.000	.286	-4.435E-5	1.709E-5
	'saline'	'amphetamine'	1.363E-5	.000	.286	-1.709E-5	4.435E-5
2	'amphetamine'	'saline'	1.937E-6	.000	.814	-1.942E-5	2.330E-5
	'saline'	'amphetamine'	-1.937E-6	.000	.814	-2.330E-5	1.942E-5

Group	(I) treatment	(J) treatment	Mean Difference (I-J)	Std. Error	Sig.[a]	95% Confidence Interval for Difference[a]	
						Lower Bound	Upper Bound
'amphetamine'	1	2	-5.646E-6	.000	.334	-1.994E-5	8.650E-6
	2	1	5.646E-6	.000	.334	-8.650E-6	1.994E-5
'saline'	1	2	9.921E-6	.000	.126	-4.375E-6	2.422E-5
	2	1	-9.921E-6	.000	.126	-2.422E-5	4.375E-6

Based on estimated marginal means

a. Adjustment for multiple comparisons: Bonferroni.

Chapter 4: Discussion

In this thesis project, we sought to study whether the changes in neural activity evoked by amphetamine administration or discontinuation were attributable to changes in arousal and locomotion.

4.1 First hypothesis

We hypothesized that a substantial amount of variance in the RSC could be accounted for by running speed and pupil size. By fitting a linear model and computing the correlation between responses and prediction (cvR^2), we found that running speed and pupil area were the two best predictors of the average neural activity changes, consistent with previous studies in the topic (Musall, Kaufman et al. 2019, Stringer, Pachitariu et al. 2019, Salkoff, Zagha et al. 2020).

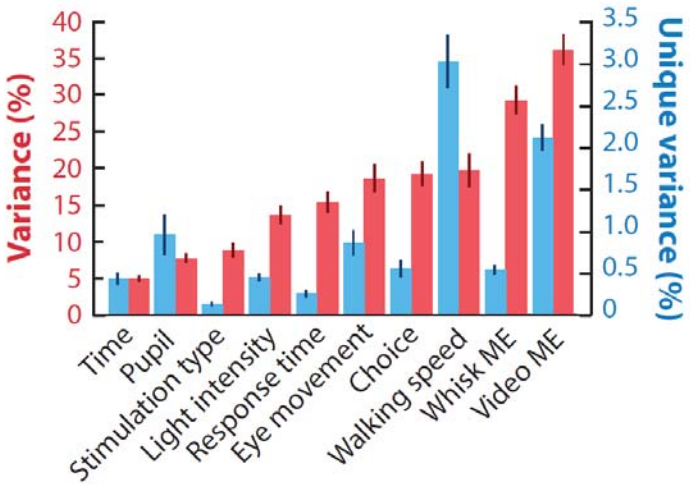

Figure 14. Movements of the face and body and behavioural measures explain a significant portion of ongoing activity in the mouse dorsal cortex (Salkoff, Zagha et al. 2020). Here, video motion energy (ME) was calculated as the sum total of absolute change in pixel intensity between adjacent video frames, whisk ME, calculated in the same manner as video ME, except for a region restricted to the main whisker pad.

Cross-validation ensured the robustness of our results: running speed explains around 32-37% of activity, whereas arousal (pupil area) makes much smaller contributions (~ 5-12%) (figure 10; table 5). This observation supports our first hypothesis, and it indicates that changes in neural activity induced by amphetamine are not independent of changes in motoric output and arousal. Instead, it reflects variations in the brain/behavioural state of the animal along interrelated dimensions (figure 6; figure S2.4). For example, movements are correlated with changes in arousal, and increases in arousal often precede movements. In addition, in mice, locomotion is always associated with whisking. These body movements are also related to changes in heart rate, respiration, gut motility, and such (McCormick, Nestvogel et al. 2020).

4.2 Second hypothesis

We hypothesized that on-board amphetamine would increase arousal and locomotion state, but it would not change the relationship between these states and neural activity. Our results support this hypothesis for arousal: systemic amphetamine administration exceeds the range of arousal values, as further evidenced by our reward-triggered changes analysis (figure 8a). We propose this increase indicates a drug-induced elevation of monoamines, especially dopamine (DA), which is expected to increase around reward. Moreover, when performing a statistical analysis to compare pupil area β-weights (slopes; regression coefficients) we did not find a significant difference in group across the on-board condition. This result means amphetamine increases neural activity by increasing arousal, and not by changing the sensitivity of neural activity to arousal.

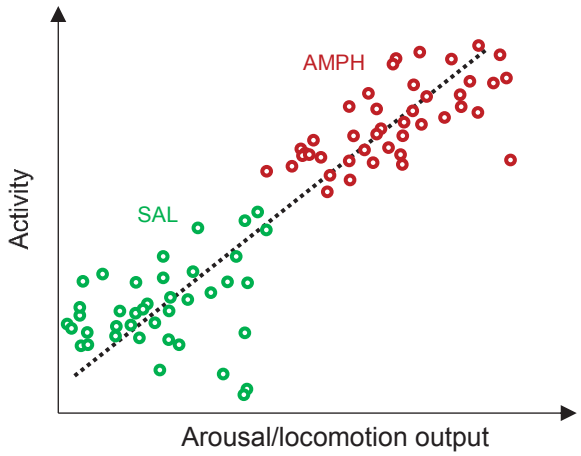

From diagram 1. Our results are consistent with one of the possible scenarios hypothesized for arousal**:** the relationship (slope) between arousal and activity is not affected by amphetamine, but amphetamine exceeds the normal range of arousal values.

The posited increase is not true for running speed. Our reward-triggered changes analysis suggests that amphetamine affects motoric output, but in the opposite direction than expected, which is consistent with the mean neural activity profile. This could be related to a dose-dependent task disengagement effect. Previous studies have shown that locomotor-enhancing effects during amphetamine administration rely on drug dose (Wilkinson, Mittleman et al. 1993, Wong, Thapa et al. 2017). Hashemnia and colleagues (2020) showed that the frequency of off-task behaviours (circling, pausing, backtracking) increase with the dose, becoming more prominent at 2.0 mg/kg. Our animals received amphetamine for ten consecutive days, and on six of those days, they received the highest dose (2.0 mg/kg). Furthermore, when comparing running speed β-weights, the statistical analysis did not show a significant difference in group across the on-board condition. This means that the relationship between locomotion and neural activity remained unaltered during amphetamine administration.

4.3 Third hypothesis

Third, we hypothesized that amphetamine discontinuation would cause hypo-arousal and decreased locomotor activity when amphetamine was 'off-board,' but the relationship between these states and neural activity would be unaltered. In contrast to what we were expecting, amphetamine discontinuation also increases arousal range values around reward delivery when amphetamine was 'off-board' (figure 8a). In fact, the estimated marginal means suggests that amphetamine 'off-board' has the highest mean. This arousal-enhancing effect during discontinuation, could result from sensitization due to multiple exposures to the drug in the past (model of chronic drug taking). Moreover, when performing a statistical analysis to compare pupil area β-weights, we did not find a significant difference in group across the off-board condition.

As mentioned before, amphetamine affects motoric output in the opposite direction than expected. In addition, our statistical analysis did not show a significant difference in group across the off-board condition when comparing running speed β-weights.

4.4 Amphetamine inverted U-shaped dose-response effect

Previous studies have shown that amphetamine induces changes in the mean firing rate of cortical neurons in a dose-dependent manner (Stone 1976, Homayoun and Moghaddam 2006, Gulley and Stanis 2010, Lapish, Balaguer-Ballester et al. 2015, Hashemnia, Euston et al. 2020). There is a significant suppression of mean firing rate with higher doses of amphetamine ($>$ 3.0 mg/kg); and a small but significant increase in the overall average firing rate with lower doses ($\sim$ 1.0 mg/kg).

Even though 2 mg/kg is a dose for which you expect an increase in neural activity, we showed a decrease, and one reason for that may be that the speed is also decreased under AMPH administration. We do not know if this is related to the specie, differences in strains of mice, differences in brain regions or because of head fixation. Nevertheless, the effects of AMPH are complex. After injection, there is a sequence of movements, then later pauses, and movement again. In general, there is variability is running speed from trial to trial. However, the distribution of the data suggests that the AMPH groups tend to pause more frequently.

4.5 The RSC role

The RSC is a major relay of hippocampal formation output to other neocortical areas. It forms a network with the prefrontal cortex (PFC), parietal cortex (PPC), and dorsomedial striatum (DMS) (Insausti, Herrero et al. 1997, Kobayashi and Amaral 2003, Aggleton 2010). We observed a remarkable correlation between neural activity and position (figure 7; figure S2.5), consistent with previous reports on the topic (Mao, Kandler et al. 2017). In particular, Mao and colleagues (2017) found a higher density of place fields and increased activity around the reward location in a similar locomotion assay as the one we used in our experiment. We noted repeated sequences of activation near the reward site, but we did not use a criterion to classify place cells. In addition, the RSC receives noradrenergic innervations from the anterior cingulate cortex (ACC), and its afferents – such as a medial prefrontal cortex (mPFC) and hippocampus – are relatively rich in dopamine receptors.

All known drugs of abuse increase norepinephrine and dopamine levels in the brain by various mechanisms. For example, cocaine binds to the dopamine transporter (DAT) and prevents transmitter reuptake (Ritz, Lamb et al. 1987). Similarly, amphetamine increases extracellular

dopamine concentration by reversing the DAT function (Fleckenstein, Volz et al. 2007). These effects on monoamine levels make the RSC useful for assessing the relationship between arousal/locomotion and neural activity, as well as the effects of amphetamine on this.

Recent studies have shown that rapid and continual changes in the arousal state of head-fixed mice are highly correlated with neocortex and hippocampus activity, and the behavioural performance of the animal (McGinley, David et al. 2015). In addition, movements and/or arousal are strongly associated with the suppression of low-frequency oscillatory activity in both cortical and subcortical structures (Reimer, Froudarakis et al. 2014, McCormick, McGinley et al. 2015, Vinck, Batista-Brito et al. 2015, Musall, Kaufman et al. 2019, Petersen 2019, Poulet and Crochet 2019, Stringer, Pachitariu et al. 2019). It is unknown whether this is due to central brain mechanisms of movement generation or because movement is linked to an increase in arousal. However, recent hypotheses suggest that both systems are intimately interlinked (Liu and Dan 2019). We do not know where the arousal/locomotor effects are taking place. Although, we believe that the RSC could be reflecting changing activity of inputs from the hippocampus, PFC, striatum, or other neocortical structures.

Even though there is still a majority of activity that cannot yet be explained by behavioural metrics, our analysis confirms the degree to which this activity is related to changes in movement during repeated amphetamine administration. This thesis provides further evidence of the importance of motoric output changes. It also highlights the need for tracking multiple movements (such as speed, whisking, eyes) when assessing the impact of drugs on neural activity. Using video recordings is a relatively easy way to accomplish this and should therefore become standard practice for physiological recordings.

Supplemental Information

S.1. Glossary

Arousal Systems and cortical activation

The brain contains internal arousal systems that stimulate cortical activation through ascending projections to the cortex; and sensory-motor responsiveness and activity through descending projections to the spinal cord. In this context, cortical activation is characterized by high frequency gamma and low frequency rhythmic theta activity (Jones, 2003).

Synchronized state

The term *synchronized state* refers to a situation in which the average population firing rate in a cortical column fluctuates strongly at a timescale of ~100 ms or slower. In such a state, low-frequency LFP power is high, although power at gamma frequencies may decrease (Harris and Thiele, 2011).

Desynchronized state

The term *desynchronized state* refers to a situation in which the population rate in a cortical column fluctuates only weakly. In such a state, low-frequency LFP power is also comparatively small. Note however that neuronal coherence at high (gamma) frequencies often actually increases in the desynchronized state, leading some authors to question the use of this term (Harris and Thiele, 2011).

S.2. Supplementary figures

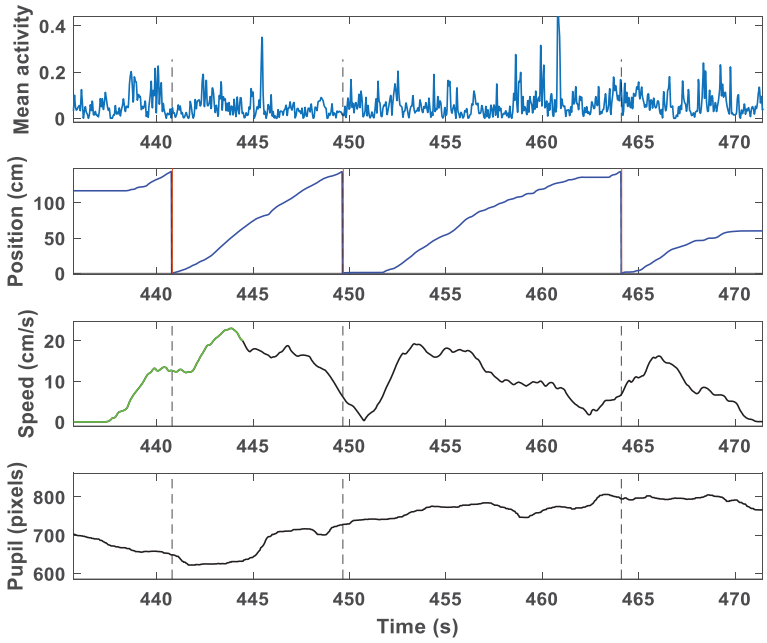

Figure S2.1. Example raw data from one experimental session (amphetamine group; on-board) showing two complete laps. (**a**) Mean neural activity (**b**) Linear position in the belt (**c**) Running speed (**d**) Pupil area trace. The dotted line corresponds to trial onset. The green section on the speed trace corresponds to a locomotion epoch: a period of 7 s in which the animal had a least 5 cm/s.

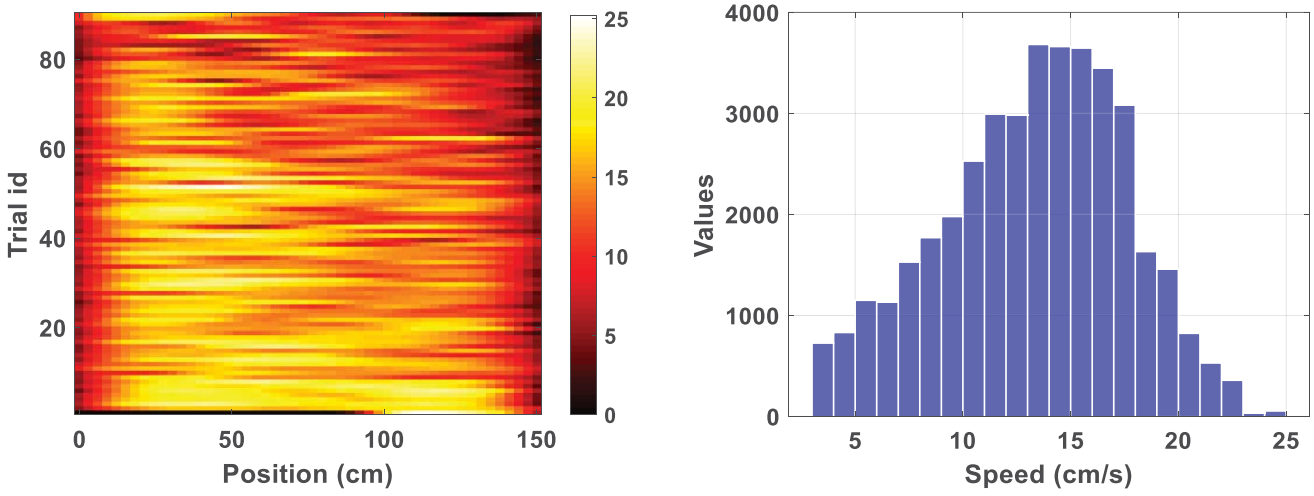

Figure S2.2. Lap running behaviour from one experimental session (amphetamine group; on-board). Left: Movement speed as a function of location for 30 consecutive laps. Right: Histogram of running speed in between reward events.

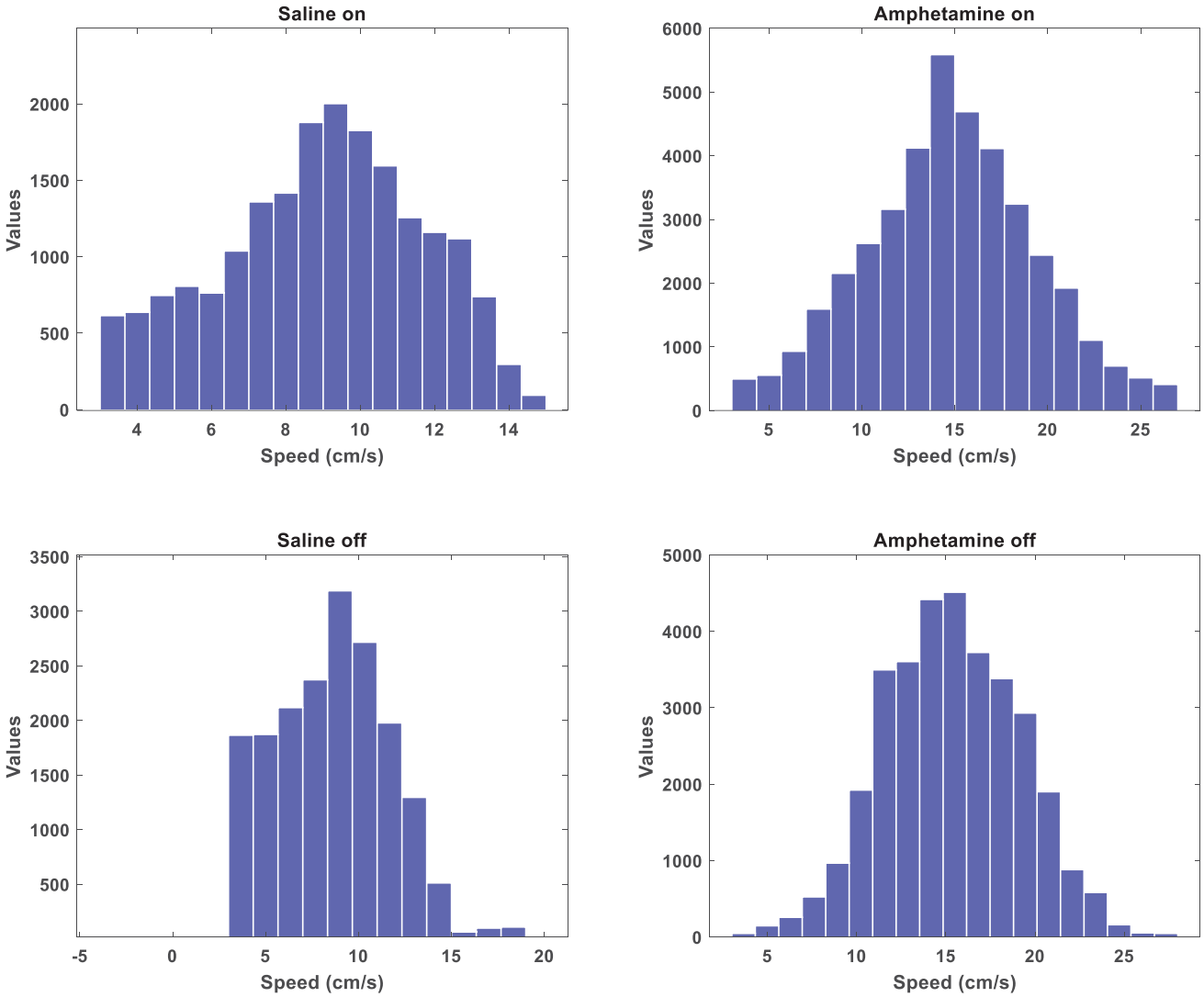

Figure S2.3: Histogram of running speed in between reward events for different treatment schedules. (a) Saline 'on-board', (b) Amphetamine 'on-board', (c) Saline 'off-board', (d) Amphetamine 'off-board'.

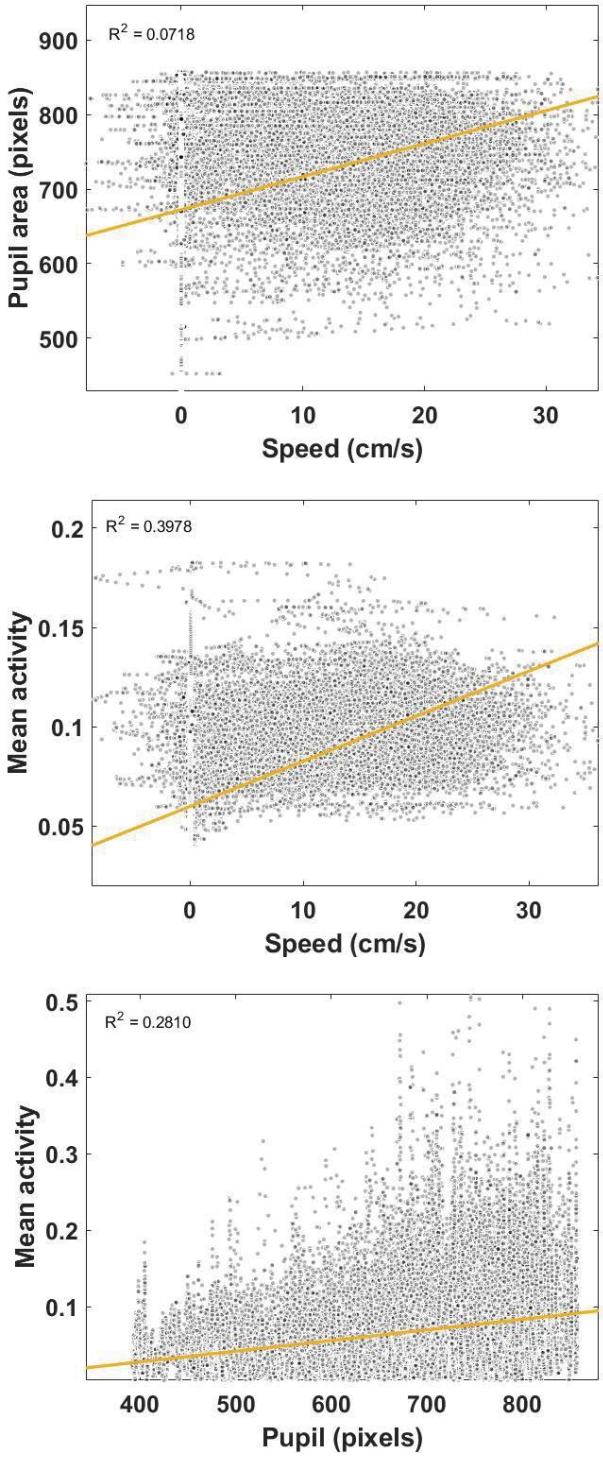

Figure S.2.4. Scatter plots for one experimental session (amphetamine group; on-board). (a) Running speed as a function of pupil area. (b) Pupil area and (c) running speed as a function of mean neural activity.

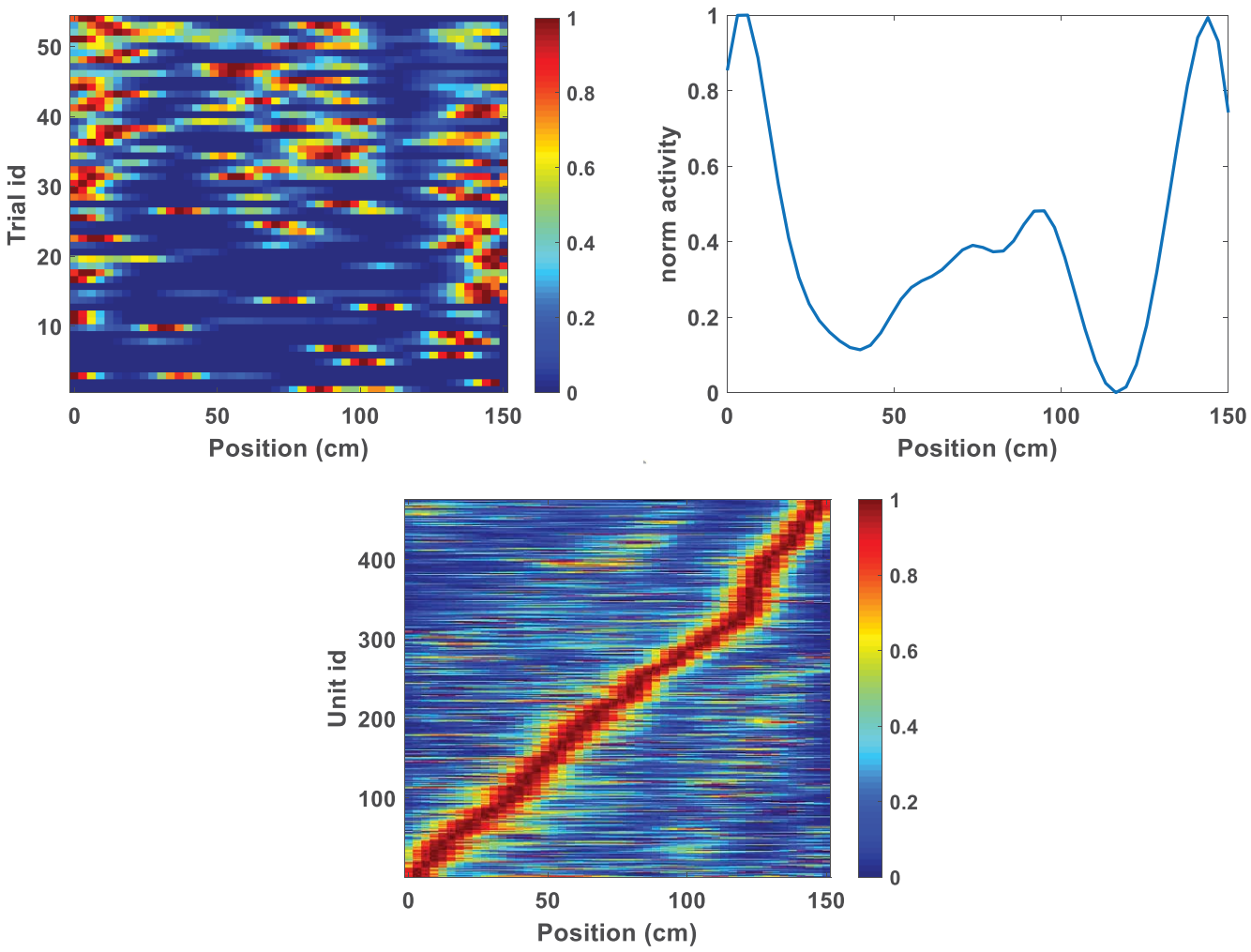

Figure S.2.5 . Location specificity of cells (amphetamine group). (a) and (b) Normalized activity of one representative cell as a function of location for 30 consecutive laps from one experimental session (amphetamine group; on-board). (c) Normalized activity as a function of location for all the 260 cells from the same experimental session.

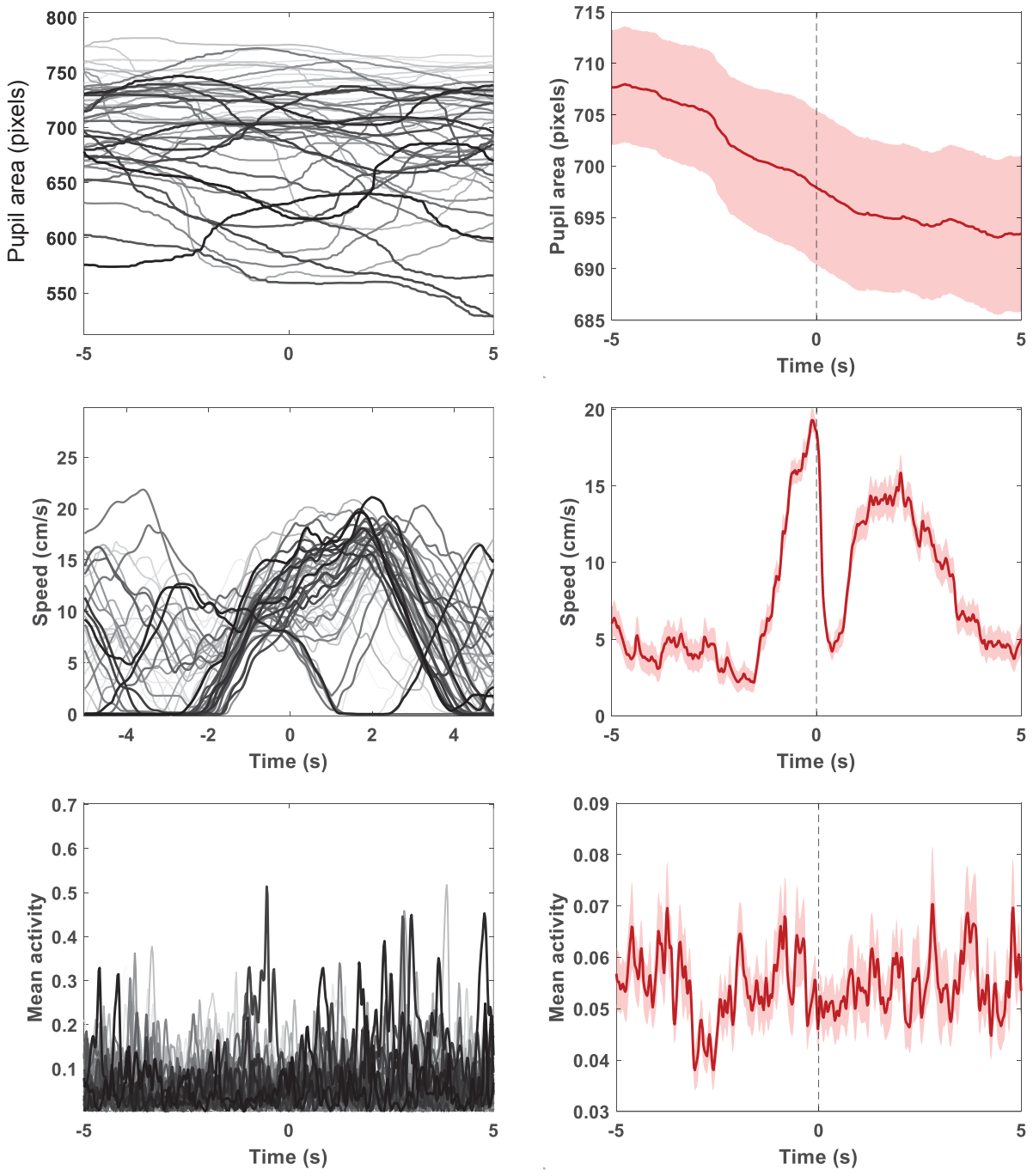

Figure S.2.6. Single session data aligned to reward (amphetamine group; on-board). Left: Data traces around reward. The color of the traces gets darker across time, and so does the line width. Right: Average reward-triggered changes trace.

References

Aggleton, J. P. (2010). "Understanding retrosplenial amnesia: insights from animal studies." Neuropsychologia **48**(8): 2328-2338.

Alexander, A. S. and D. A. Nitz (2015). "Retrosplenial cortex maps the conjunction of internal and external spaces." Nature neuroscience **18**(8): 1143-1151.

Alexander, A. S. and D. A. Nitz (2017). "Spatially periodic activation patterns of retrosplenial cortex encode route sub-spaces and distance traveled." Current Biology **27**(11): 1551-1560. e1554.

Alnæs, D., et al. (2014). "Pupil size signals mental effort deployed during multiple object tracking and predicts brain activity in the dorsal attention network and the locus coeruleus." Journal of vision **14**(4): 1-1.

Belujon, P., et al. (2016). "Withdrawal from acute amphetamine induces an amygdala-driven attenuation of dopamine neuron activity: reversal by ketamine." Neuropsychopharmacology **41**(2): 619-627.

Bennett, C., et al. (2013). "Subthreshold mechanisms underlying state-dependent modulation of visual responses." Neuron **80**(2): 350-357.

Bradley, M. M., et al. (2008). "The pupil as a measure of emotional arousal and autonomic activation." Psychophysiology **45**(4): 602-607.

Cenquizca, L. A. and L. W. Swanson (2007). "Spatial organization of direct hippocampal field CA1 axonal projections to the rest of the cerebral cortex." Brain research reviews **56**(1): 1-26.

Chen, L. L., et al. (1994). "Head-direction cells in the rat posterior cortex." Experimental brain research **101**(1): 8-23.

Cho, J. and P. E. Sharp (2001). "Head direction, place, and movement correlates for cells in the rat retrosplenial cortex." Behavioral neuroscience **115**(1): 3.

Cohen, M. R. and J. H. Maunsell (2009). "Attention improves performance primarily by reducing interneuronal correlations." Nature neuroscience **12**(12): 1594-1600.

Contreras, D., et al. (1996). "Mechanisms of long-lasting hyperpolarizations underlying slow sleep oscillations in cat corticothalamic networks." The Journal of physiology **494**(1): 251-264.

Contreras, E. J. B., et al. (2013). "Formation and reverberation of sequential neural activity patterns evoked by sensory stimulation are enhanced during cortical desynchronization." Neuron **79**(3): 555-566.

Crochet, S. and C. C. Petersen (2006). "Correlating whisker behavior with membrane potential in barrel cortex of awake mice." Nature neuroscience **9**(5): 608-610.

Czajkowski, R., et al. (2014). "Encoding and storage of spatial information in the retrosplenial cortex." Proceedings of the National Academy of Sciences **111**(23): 8661-8666.

de Gee, J. W., et al. (2014). "Decision-related pupil dilation reflects upcoming choice and individual bias." Proceedings of the National Academy of Sciences **111**(5): E618-E625.

Destexhe, A., et al. (1999). "Spatiotemporal analysis of local field potentials and unit discharges in cat cerebral cortex during natural wake and sleep states." Journal of Neuroscience **19**(11): 4595-4608.

Einhauser, W., et al. (2010). "Pupil dilation betrays the timing of decisions." Frontiers in human neuroscience **4**: 18.

Faraone, S. V. (2018). "The pharmacology of amphetamine and methylphenidate: relevance to the neurobiology of attention-deficit/hyperactivity disorder and other psychiatric comorbidities." Neuroscience & Biobehavioral Reviews **87**: 255-270.

Fleckenstein, A. E., et al. (2007). "New insights into the mechanism of action of amphetamines." Annu. Rev. Pharmacol. Toxicol. **47**: 681-698.

Friedrich, J., et al. (2017). "Fast online deconvolution of calcium imaging data." PLoS computational biology **13**(3): e1005423.

Gentet, L. J., et al. (2010). "Membrane potential dynamics of GABAergic neurons in the barrel cortex of behaving mice." Neuron **65**(3): 422-435.

Gilzenrat, M. S., et al. (2010). "Pupil diameter tracks changes in control state predicted by the adaptive gain theory of locus coeruleus function." Cognitive, Affective, & Behavioral Neuroscience **10**(2): 252-269.

Gulley, J. M. and J. J. Stanis (2010). "Adaptations in medial prefrontal cortex function associated with amphetamine-induced behavioral sensitization." Neuroscience **166**(2): 615-624.

Haber, S., et al. (1981). "A primate analogue of amphetamine-induced behaviors in humans." Biological psychiatry.

Harris, K. D. and A. Thiele (2011). "Cortical state and attention." Nature reviews neuroscience **12**(9): 509-523.

Hashemnia, S., et al. (2020). "Amphetamine reduces reward encoding and stabilizes neural dynamics in rat anterior cingulate cortex." ELife **9**: e56755.

Hess, E. H. and J. M. Polt (1960). "Pupil size as related to interest value of visual stimuli." Science **132**(3423): 349-350.

Hess, E. H. and J. M. Polt (1964). "Pupil size in relation to mental activity during simple problem-solving." Science **143**(3611): 1190-1192.

Hoeks, B. and W. J. Levelt (1993). "Pupillary dilation as a measure of attention: A quantitative system analysis." Behavior Research Methods, Instruments, & Computers **25**(1): 16-26.

Homayoun, H. and B. Moghaddam (2006). "Progression of cellular adaptations in medial prefrontal and orbitofrontal cortex in response to repeated amphetamine." Journal of Neuroscience **26**(31): 8025-8039.

Insausti, R., et al. (1997). "Entorhinal cortex of the rat: cytoarchitectonic subdivisions and the origin and distribution of cortical efferents." Hippocampus **7**(2): 146-183.

Iriki, A., et al. (1996). "Attention-induced neuronal activity in the monkey somatosensory cortex revealed by pupillometrics." Neuroscience Research **25**(2): 173-181.

Jones, B. E. (2003). "Arousal systems." Front Biosci **8**(5): 438-451.

Joshi, S., et al. (2016). "Relationships between pupil diameter and neuronal activity in the locus coeruleus, colliculi, and cingulate cortex." Neuron **89**(1): 221-234.

Kahneman, D. and J. Beatty (1966). "Pupil diameter and load on memory." Science **154**(3756): 1583-1585.

Karabatsos, G. (2018). "Marginal maximum likelihood estimation methods for the tuning parameters of ridge, power ridge, and generalized ridge regression." Communications in Statistics-Simulation and Computation **47**(6): 1632-1651.

Kobayashi, Y. and D. G. Amaral (2003). "Macaque monkey retrosplenial cortex: II. Cortical afferents." Journal of Comparative Neurology **466**(1): 48-79.

Lapish, C. C., et al. (2015). "Amphetamine exerts dose-dependent changes in prefrontal cortex attractor dynamics during working memory." Journal of Neuroscience **35**(28): 10172-10187.

Liu, D. and Y. Dan (2019). "A motor theory of sleep-wake control: arousal-action circuit." Annual review of neuroscience **42**: 27-46.

Mao, D., et al. (2017). "Sparse orthogonal population representation of spatial context in the retrosplenial cortex." Nature communications **8**(1): 1-9.

McAdams, C. J. and J. H. Maunsell (1999). "Effects of attention on the reliability of individual neurons in monkey visual cortex." Neuron **23**(4): 765-773.

McCormick, D. A. and T. Bal (1997). "Sleep and arousal: thalamocortical mechanisms." Annual review of neuroscience **20**(1): 185-215.

McCormick, D. A., et al. (2015). "Brain state dependent activity in the cortex and thalamus." Current opinion in neurobiology **31**: 133-140.

McCormick, D. A., et al. (2020). "Neuromodulation of brain state and behavior." Annual review of neuroscience **43**: 391-415.

McDougal, D. H. and P. D. Gamlin (2015). "Autonomic control of the eye." Comprehensive Physiology **5**(1): 439.

McGinley, M. J., et al. (2015). "Cortical membrane potential signature of optimal states for sensory signal detection." Neuron **87**(1): 179-192.

Mitchell, J. F., et al. (2009). "Spatial attention decorrelates intrinsic activity fluctuations in macaque area V4." Neuron **63**(6): 879-888.

Murphy, P. R., et al. (2011). "Pupillometry and P3 index the locus coeruleus–noradrenergic arousal function in humans." Psychophysiology **48**(11): 1532-1543.

Musall, S., et al. (2019). "Single-trial neural dynamics are dominated by richly varied movements." Nature neuroscience **22**(10): 1677-1686.

Niell, C. M. and M. P. Stryker (2010). "Modulation of visual responses by behavioral state in mouse visual cortex." Neuron **65**(4): 472-479.

Pachitariu, M., et al. (2017). "Suite2p: beyond 10,000 neurons with standard two-photon microscopy." BioRxiv.

Paulson, P. E., et al. (1991). "Time course of transient behavioral depression and persistent behavioral sensitization in relation to regional brain monoamine concentrations during amphetamine withdrawal in rats." Psychopharmacology **103**(4): 480-492.

Petersen, C. C. (2019). "Sensorimotor processing in the rodent barrel cortex." Nature reviews neuroscience **20**(9): 533-546.

Polack, P.-O., et al. (2013). "Cellular mechanisms of brain state–dependent gain modulation in visual cortex." Nature neuroscience **16**(9): 1331-1339.

Poock, G. K. (1973). "Information processing vs pupil diameter." Perceptual and motor skills **37**(3): 1000-1002.

Poulet, J. F. and S. Crochet (2019). "The cortical states of wakefulness." Frontiers in systems neuroscience **12**: 64.

Reimer, J., et al. (2014). "Pupil fluctuations track fast switching of cortical states during quiet wakefulness." Neuron **84**(2): 355-362.

Reimer, J., et al. (2016). "Pupil fluctuations track rapid changes in adrenergic and cholinergic activity in cortex." Nature communications **7**(1): 1-7.

Ritz, M. C., et al. (1987). "Cocaine receptors on dopamine transporters are related to self-administration of cocaine." Science **237**(4819): 1219-1223.

Robinson, T. E. and B. Kolb (1997). "Persistent structural modifications in nucleus accumbens and prefrontal cortex neurons produced by previous experience with amphetamine." Journal of Neuroscience **17**(21): 8491-8497.

Saleem, A. B., et al. (2013). "Integration of visual motion and locomotion in mouse visual cortex." Nature neuroscience **16**(12): 1864-1869.

Salkoff, D. B., et al. (2020). "Movement and performance explain widespread cortical activity in a visual detection task." Cerebral Cortex **30**(1): 421-437.

Smith, D. M., et al. (2012). "Complimentary roles of the hippocampus and retrosplenial cortex in behavioral context discrimination." Hippocampus **22**(5): 1121-1133.

Steriade, M. (1996). "Arousal--Revisiting the Reticular Activating System." Science **272**(5259): 225-225.

Steriade, M., et al. (1993). "Thalamocortical oscillations in the sleeping and aroused brain." Science **262**(5134): 679-685.

Steriade, M., et al. (2001). "Natural waking and sleep states: a view from inside neocortical neurons." Journal of neurophysiology **85**(5): 1969-1985.

Stone, T. (1976). "Responses of neurones in the cerebral cortex and caudate nucleus to amantadine, amphetamine and dopamine." British journal of pharmacology **56**(1): 101.

Stringer, C. and M. Pachitariu (2019). "Computational processing of neural recordings from calcium imaging data." Current opinion in neurobiology **55**: 22-31.

Stringer, C., et al. (2019). "Spontaneous behaviors drive multidimensional, brainwide activity." Science **364**(6437).

Sugar, J., et al. (2011). "The retrosplenial cortex: intrinsic connectivity and connections with the (para) hippocampal region in the rat. An interactive connectome." Frontiers in neuroinformatics **5**: 7.

Sutherland, R., et al. (1988). "Contributions of cingulate cortex to two forms of spatial learning and memory." Journal of Neuroscience **8**(6): 1863-1872.

van Groen, T. and J. M. Wyss (1992). "Connections of the retrosplenial dysgranular cortex in the rat." Journal of Comparative Neurology **315**(2): 200-216.

Van Groen, T. and J. M. Wyss (2003). "Connections of the retrosplenial granular b cortex in the rat." Journal of Comparative Neurology **463**(3): 249-263.

Vann, S. D. and J. P. Aggleton (2005). "Selective dysgranular retrosplenial cortex lesions in rats disrupt allocentric performance of the radial-arm maze task." Behavioral neuroscience **119**(6): 1682.

Vedder, L. C., et al. (2017). "Retrosplenial cortical neurons encode navigational cues, trajectories and reward locations during goal directed navigation." Cerebral Cortex **27**(7): 3713-3723.

Vinck, M., et al. (2015). "Arousal and locomotion make distinct contributions to cortical activity patterns and visual encoding." Neuron **86**(3): 740-754.

Wilkinson, L. S., et al. (1993). "Enhancement of amphetamine-induced locomotor activity and dopamine release in nucleus accumbens following excitotoxic lesions of the hippocampus." Behavioural brain research **55**(2): 143-150.

Wong, S. A., et al. (2017). "Opposing effects of acute and chronic d-amphetamine on decision-making in rats." Neuroscience **345**: 218-228.

Wyass, J. M. and T. Van Groen (1992). "Connections between the retrosplenial cortex and the hippocampal formation in the rat: a review." Hippocampus **2**(1): 1-11.

Zagha, E., et al. (2013). "Motor cortex feedback influences sensory processing by modulating network state." Neuron **79**(3): 567-578.

Zhou, M., et al. (2014). "Scaling down of balanced excitation and inhibition by active behavioral states in auditory cortex." Nature neuroscience **17**(6): 841-850.